Petrology of the Welded Tuff of Devine Canyon, Southeastern Oregon

GEOLOGICAL SURVEY PROFESSIONAL PAPER 797

Petrology of the Welded Tuff of Devine Canyon, Southeastern Oregon

By ROBERT C. GREENE

GEOLOGICAL SURVEY PROFESSIONAL PAPER 797

UNITED STATES GOVERNMENT PRINTING OFFICE, WASHINGTON : 1973

UNITED STATES DEPARTMENT OF THE INTERIOR

ROGERS C. B. MORTON, *Secretary*

GEOLOGICAL SURVEY

V. E. McKelvey, *Director*

Library of Congress catalog-card No. 73-600097

For sale by the Superintendent of Documents, U.S. Government Printing Office
Washington, D.C. 20402 – Price 65 cents domestic postpaid or 45 cents GPO Bookstore
Stock Number 2401-00331

CONTENTS

ILLUSTRATIONS

TABLES

PETROLOGY OF THE WELDED TUFF OF DEVINE CANYON, SOUTHEASTERN OREGON

By ROBERT C. GREENE

ABSTRACT

The welded tuff of Devine Canyon, the most widespread ash-flow tuff in southeastern Oregon, is centered around the Harney Basin lowland south of Burns; it originally covered about 7,200 square miles and had a volume of over 47 cubic miles. Its age is early Pliocene, about 9 million years. Thickness ranges from a few feet to over 100 feet. Most sections under 35 feet thick are entirely vitric; thicker sections are devitrified but have a vitric base.

The distribution of the tuff suggests that the source area lies buried beneath Quaternary sediments in the northwest part of the Harney Basin lowland. Downwarping of this lowland may be related to the expulsion of magma from beneath to form the Devine Canyon and other welded tuff sheets.

Phenocrysts are mostly alkali feldspar ($Or_{42}Ab_{58}$) and quartz with minor iron-rich pyroxene. Alkali feldspar phenocryst content ranges from 1 to 29 percent and increases markedly upwards in most sections.

Analyses of 14 samples show that the devitrified tuff is uniform in composition. Unlike the welded tuffs of southern Nevada, samples that are rich in phenocrysts are similar in composition to samples that are not; this fact indicates that phenocrysts crystallized in the magma chamber without significant crystal settling. A water pressure of between 800 and 1,800 bars during phenocryst crystallization is indicated by comparison with the experimental data of Tuttle and Bowen. Resorption of phenocrysts at all levels in the magma indicates reduction in water pressure prior to ash-flow eruption, probably by venting of water vapor plus minor air-fall tuff. Eruption onto a very flat plain produced an exceptionally widespread but relatively thin tuff sheet.

INTRODUCTION

The study of ash-flow tuffs has gained considerable impetus in recent years, particularly through the work of Smith (1960a, b) and Ross and Smith (1961). Smith has described with clarity and precision the characteristics of welding and crystallization zones, and the nomenclature he established has been widely accepted. Work at the Atomic Energy Commission Nevada Test Site in southern Nevada has resulted in the mapping and description of many heretofore unknown ash-flow tuffs (Hinrichs and Orkild, 1961; Lipman and Christiansen, 1964; Lipman and others, 1966; Byers and others, 1968). Many of these tuffs show striking compositional zonation, commonly from phenocryst-poor rhyolite at the base to phenocryst-rich quartz latite at the top.

The welded tuff of Devine Canyon in southeastern Oregon (fig. 1), is a very widespread but thin unit. Like those of southern Nevada, it is zoned from a phenocryst-poor base to a phenocryst-rich upper part. However, the bulk composition is uniform, and phenocrysts appear to have crystallized in place in the preeruption magma chamber without settling appreciably. Eruption of the magma produced a tuff zoned as to phenocryst content, but not recording significant magmatic differentiation.

TOPOGRAPHIC AND GEOLOGIC SETTING

The area underlain by the welded tuff of Devine Canyon is part of the "High Lava Plains" section of Oregon (Baldwin, 1959; Walker, 1969, p. 77). It is a region of high plateaus, locally broken into tilted fault blocks and cut in places by deep canyons. Rocks are mainly flat-lying to gently tilted Miocene, Pliocene, and Quaternary volcanic and continental sedimentary rocks, with local occurrences of pre-Tertiary rocks. In the central part of the region is a basin floored mostly with Quaternary lake sediments, herein referred to as the Harney Basin Lowland (fig. 1).

Numerous ash-flow tuffs have been recognized in southeastern Oregon (fig. 2; Walker, 1970). All are of late Miocene or Pliocene age (table 1). The welded tuffs of Devine Canyon, Double O Ranch, and the Trout Creek Mountains are the most voluminous and complex; the others are much smaller. Welded tuffs of Devine Canyon, Prater Creek, and Double O Ranch form an important threefold sequence on the north side of the Harney Basin lowland (north of Burns). All three are well exposed in Devine Canyon, Poison Creek, and Silvies River canyon (Greene, 1972; Greene and others, 1972).

ACKNOWLEDGMENTS

The writer gratefully acknowledges the contribution of mapping by George W. Walker, both in the Adel and the south-central part of the Burns 1° by 2° quad-

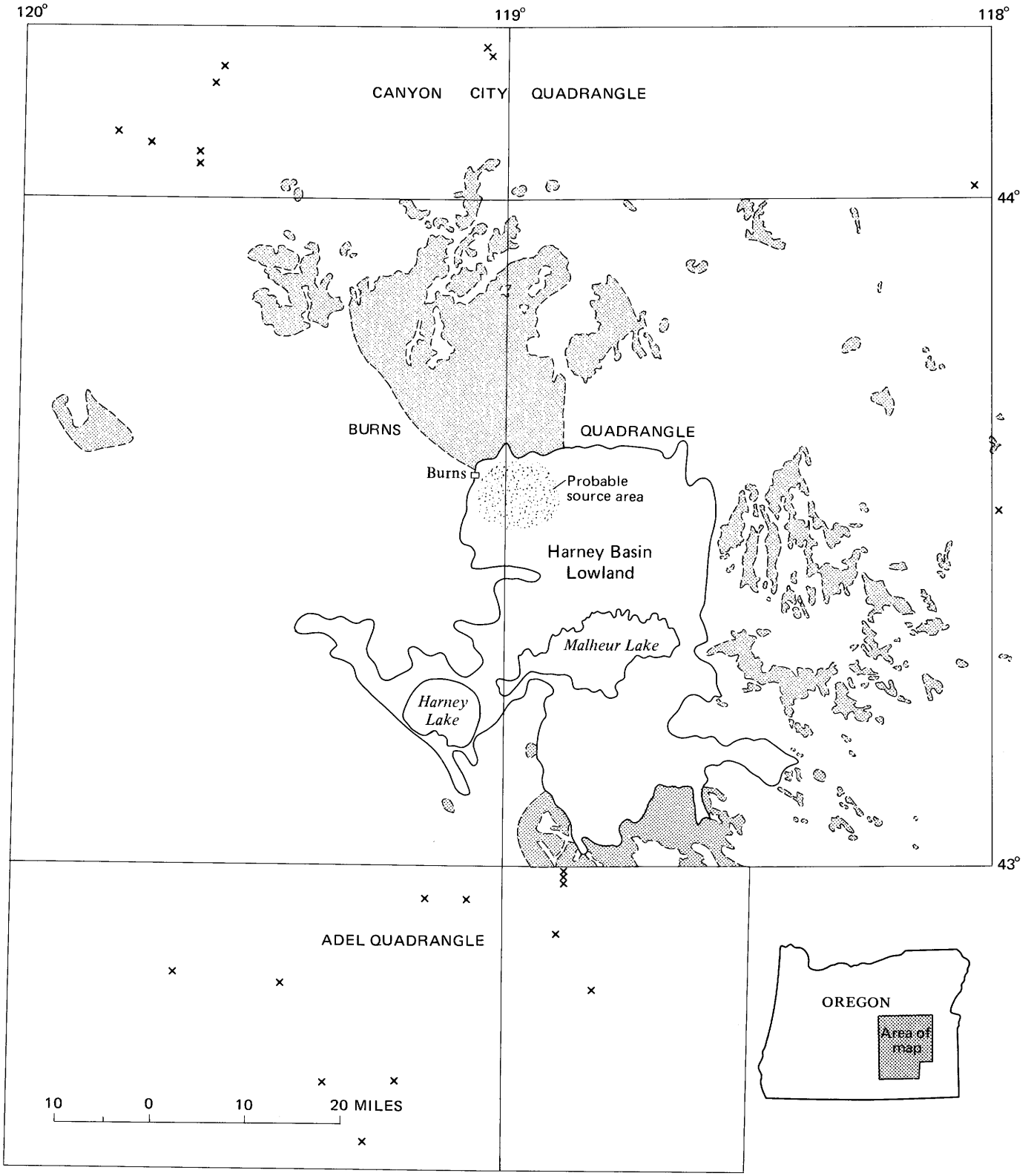

FIGURE 1.—Outcrop area, with minimal downdip projection, of welded tuff of Devine Canyon.

rangles. R. C. Erd supplied powder and single-crystal X-ray data for the pyroxene from sample 148–3. Potassium-argon dates were determined by J. C. Engels, M. A. Lanphere, and J. C. Von Essen.

TABLE 1.—*Major welded tuff units in southeastern Oregon*

Name and (or) location[1]	Age (m.y)	Age reference	Map reference
Pliocene			
West side Hampton Butte	3.6	Walker (1970, p. 102)	Walker and others (1967).
Rattlesnake Formation	6.4	Evernden and others (1964)	Brown and Thayer (1966).
Double O Ranch	6.8	Greene and others (1972)	Walker (1963), Walker and Repenning (1965), Walker and others (1967), Greene and others (1972), reconnaissance by G. W. Walker (1968–70) and D. A. Swanson (1968).
Prater Creek		Greene and others (1972)	Greene and others (1972).
Wagontire		G. W. Walker (oral commun., 1969)	Walker and others (1967), Greene and others (1972).
Devine Canyon	9.2	This paper	Walker and Repenning (1965), Brown and Thayer (1966), Greene and others (1972), reconnaissance by G. W. Walker (1968–70).
Buchanan		Greene and others (1972)	Greene and others (1972).
South Fork Crooked River		G. W. Walker (oral commun., 1969)	Walker and others (1967).
Wildcat Creek Welded Ash-flow Tuff of Kittleman and others (1965).		Kittleman and others (1965)	Kittleman and others (1967).
Miocene			
Trout Creek		G. W. Walker (oral commun., 1969)	Walker and Repenning (1965).
Dinner Creek Welded Tuff		Kittleman and others (1965)	Kittleman and others (1967, Haddock (1967), reconnaissance by G. W. Walker (1969–70).
Leslie Gulch Ash-flow Member of Sucker Creek Formation of Kittleman and others (1965).		Kittleman and others (1965)	Kittleman and others (1967).

[1]Welded tuffs are arranged in approximate stratigraphic order. Relative position within groups is uncertain.

GENERAL FEATURES

The welded tuff of Devine Canyon consists of soda and alkali rhyolites, as defined by Rittmann (1952, p. 81). The tuff sheet contains porous vitric, dense vitric, dense devitrified, and vapor phase zones, much as described by Smith (1960b) and Ross and Smith (1961). Most of the tuff is strongly welded. Lithophysae are absent. Groundmass consists of shards and pumice, both of which are variously flattened and stretched, so that the rocks have a wide range of densities. Phenocrysts are alkali feldspar and quartz, with trace amounts of pyroxene (ferrohedenbergite), ilmenite, and magnetite. Rock fragments are sparse and are mostly andesite.

This tuff forms a simple cooling unit (Ross and Smith, 1961). It seems to be composed of a single ash flow, although local obscure partings suggest the possibility of more than one flow.

The original extent and volume of the tuff were calculated from an isopach map (fig. 3), which was prepared on the basis of outcrop pattern (fig. 1) and thickness data. The zero isopach shows the inferred original extent of the tuff. The tuff must have covered an area of about 7,200 square miles (18,600 sq km) and had a total volume of about 47 cubic miles (195 cu km). This places it in order 6 or 7 of Smith (1960a), which suggests that it originated in a subsidence structure.

AGE

Potassium-argon dates on the tuff range from 8.5 to 9.7 m.y. (table 2); all five dates were made on alkali feldspar phenocrysts from fresh vitric tuff. The determinations on samples from Diamond and Catlow Valley, however, were done in different laboratories while dating techniques were still being developed. The average of the other three is 9.2 m.y., and the total deviation only 0.6 m.y.

VITRIC TUFF

Vitric tuff occurs in the basal and, rarely, the upper parts of the tuff sheet and is the dominant type near the outer margin. It varies considerably in density. Much is moderately dense (2.0–2.2) and medium to light gray (*N*5–*N*7), or medium to light greenish to olive gray (5*GY* 6–8/1, 5*Y* 6–8/1), more rarely light brownish gray (5*YR* 6/1). Alternating lenticular color bands of darker and lighter values of the same hue are common. The weathered surface of this type of tuff is slightly darker or browner than a fresh surface, but the tuff remains coherent even after moderate weathering. Fracture is planar to conchoidal (fig. 4).

Denser (2.2–2.35) vitric tuff is generally greenish gray (5*GY* 5–6/1) and in places is streaked with light olive or light brownish gray (5*Y*–5*YR* 6/1). Its texture is commonly perlitic. This tuff has hackly fracture and weathers to small bits.

Vitric tuff of low density (1.1–2.0) is light to very light gray (*N*7–8) and is visibly porous. The least dense rock crumbles when touched, breaking down to individual shards and pumice lumps. This incoherent rock was found only at the Drinkwater Pass section (fig. 5).

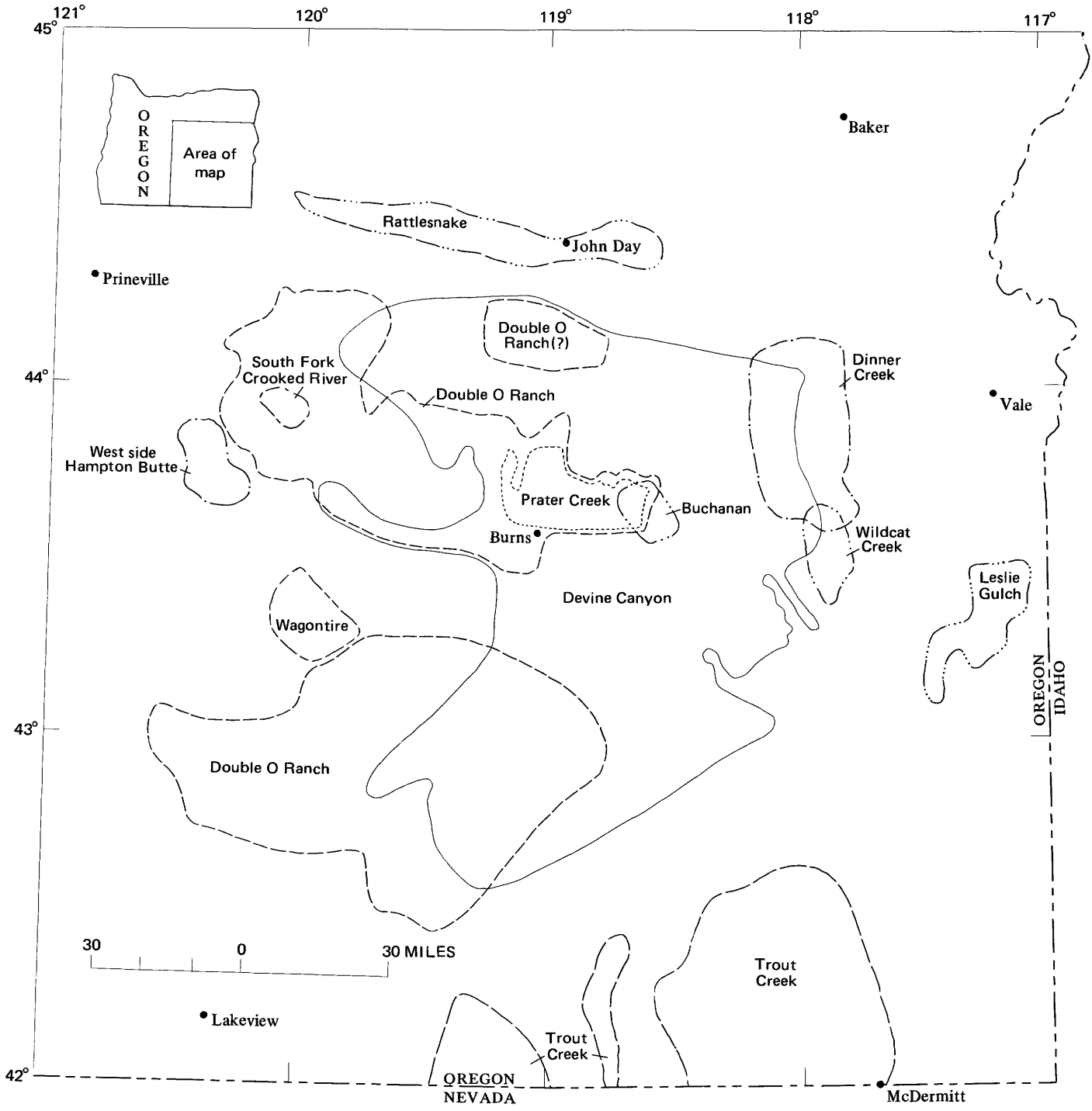

FIGURE 2.—Location and extent of major welded tuff sheets of southeastern Oregon (see table 1 for relative ages and references).

Glass shards in a matrix of glass "dust" characterize the groundmass of the vitric tuffs (fig. 6). The shards are generally colorless and the matrix is either uniform pale brown (fig. 9) or irregular pale to dark brown (figs. 7, 8). Degree of flattening and stretching of the shards is proportional to the density of the tuff. Shards are severely flattened near phenocrysts, where they "flow" in smooth parallel streaks around the crystal (figs. 7–9). Minute voids between shards account for much of the porosity; in places, visible pores are sparse in rocks of relatively low density (fig. 7, specimen 153–4, density=1.833). The progressive compaction and flattening of the shards in the vitric tuffs is illustrated in a sequence of photomicrographs (figs. 6–9).

Pumice occurs in a variety of forms. In tuffs of low density it occurs as highly porous ragged to lenticular

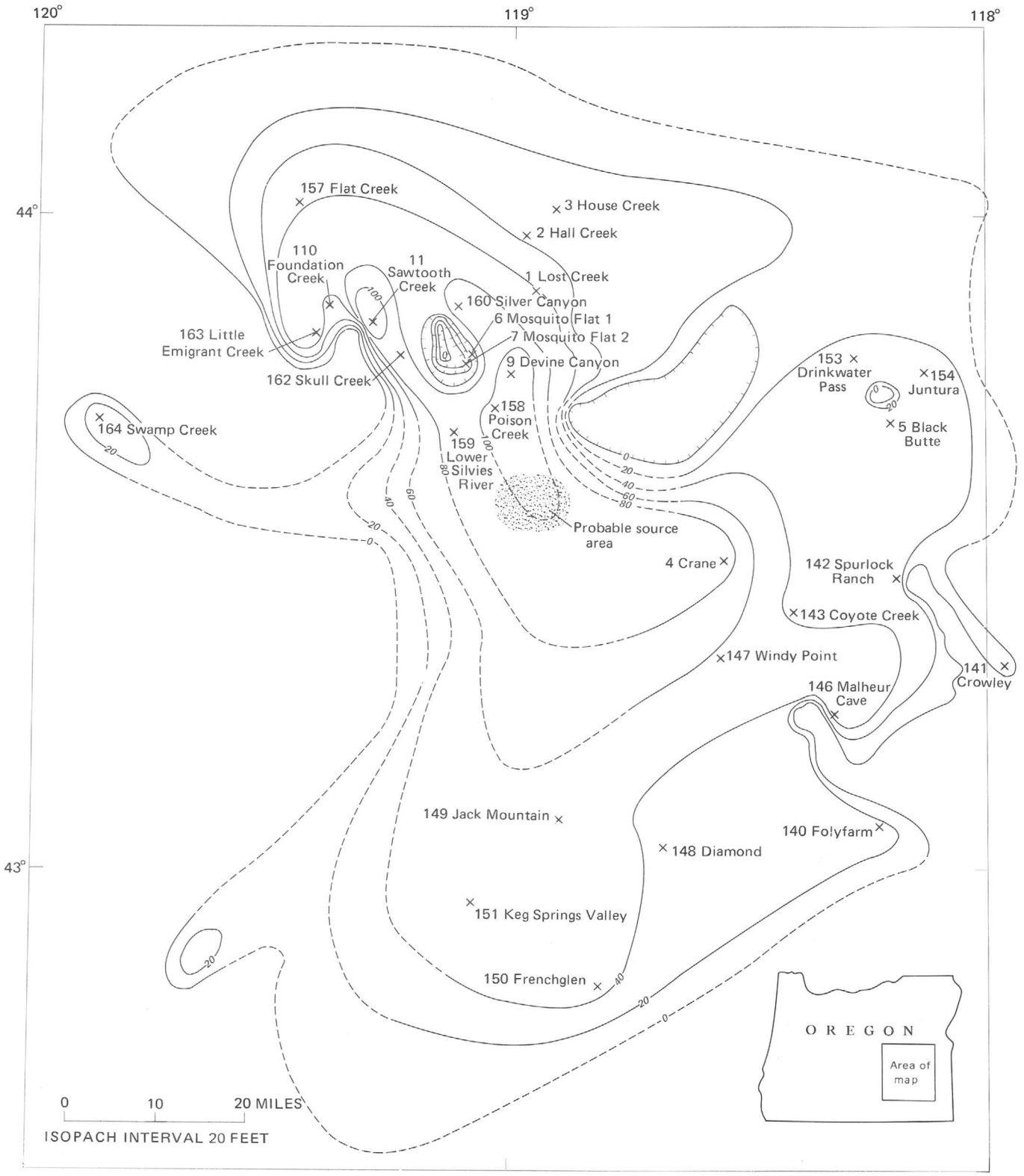

FIGURE 3.—Isopach map of welded tuff of Devine Canyon, showing locations of measured sections. Lines dashed where uncertain.

fragments (fig. 10). In dense tuffs, it appear as pale-brown to colorless glass in lenses or "knots" of small to nil porosity.

Phenocrysts of alkali feldspar and quartz vary in amount from rare to very abundant. Nearly every thin section studied contains a few quartz and feldspar

TABLE 2.—*Potassium-argon dates on the welded tuff of Devine Canyon*

Age (m.y)	Sample No.	Location	Section, township, range	Analyst and year (reference)
8.5±0.3	GWW–176–62	Diamond	Sec. 34, T. 29 S., R. 33 E.	Kistler, Whitehead, and Schlocker (1963), *in* Greene and others (1972).
8.9	KA122S	Drinkwater Pass	Sec. 34, T. 20 S., R. 36 E.	Evernden (1964), *in* Evernden and others (1964).
9.21±0.50	RCG–248–66	Devine Canyon	Sec. 16, T. 21 S., R. 31 E.	Von Essen (1967), *in* Greene and others (1972).
9.45± .21	GWW–16–65	Swamp Creek	Sec. 1, T. 22 S., R. 23 E.	Engles and Lanphere (1966), *in* Greene and others (1972).
9.7±0.3	GWW–140–61	Catlow Valley	Sec. 26, T. 34 S., R. 29 E.	Kistler and Walthal (1963), *in* Walker and Repenning (1965).

FIGURE 4.—Juntura section. Tuffaceous sediments at base of exposure, followed by 1 foot of bedded pumice. Welded tuff, 23 feet thick, all moderately dense vitric, somewhat brecciated at base. Platy horizontal joints dominant, suggestion of spheroidal weathering forms.

phenocrysts that are euhedral (figs. 8, 15, 16), but the vast majority of phenocrysts show some rounding or embayment (figs. 7, 9, 14, 16, 17). Resorption effects show no apparent relation to position in the section, or to abundance of phenocrysts. A few percent of the phenocrysts in each thin section are broken fragments (figs. 9, 15, 16). Alkali feldspar is generally recognized by cleavage and twinning, but some is distinguished from quartz only with difficulty.

Phenocrysts of ferro-magnesian minerals consist of very rare pyroxene and opaque minerals. Pyroxene crystals (fig. 8) are pleochroic in green and yellow green. Where unaltered, magnetite and ilmenite crystals are opaque and steel gray in reflected light; where

FIGURE 5.—Drinkwater Pass section, 34½ feet thick. Tuff is all of low density, densest in middle (fig. 20, sec. 153). Horizontal joints produce slabs in middle and upper parts; lower part of very low density disintegrates to small lumps, producing notch at base.

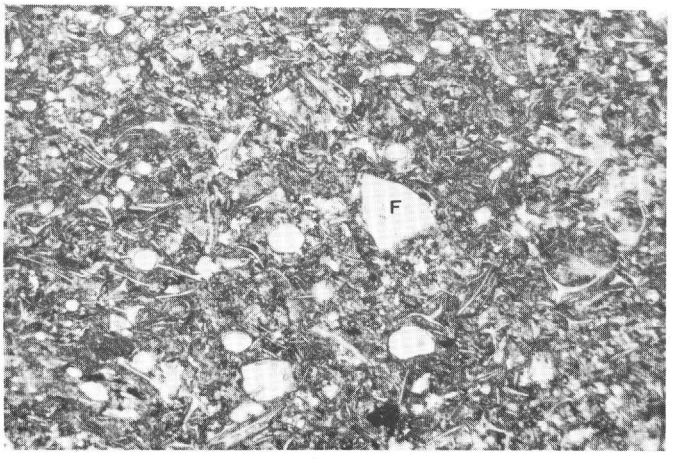

FIGURE 6.—Photomicrograph of tuff from section 153, specimen 1. Nonwelded vitric, crystal-poor basal part of section, round pores resemble vesicles. One phenocryst of feldspar (F) in right center. Plain light.

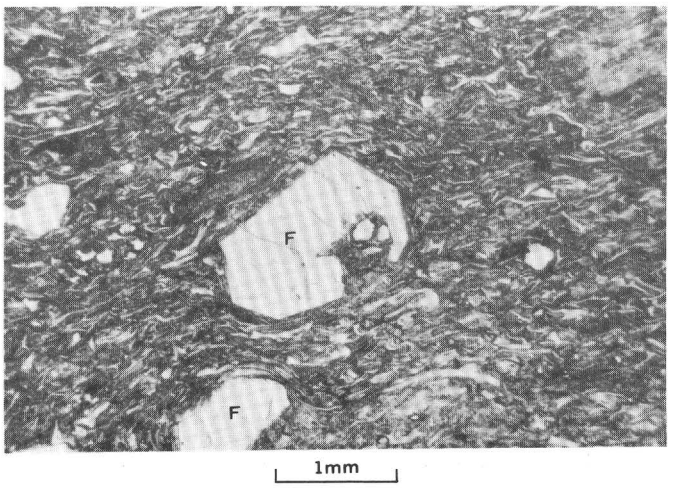

FIGURE 7.—Photomicrograph of tuff from section 154, specimen 4. Slightly welded vitric tuff, shards somewhat flattened, bend around phenocrysts. Euhedral alkali feldspar phenocryst (F) in center notably embayed; alkali feldspar phenocryst at bottom somewhat rounded. Ragged end of pumice lump in upper right corner. Plain light.

altered, they are partly decomposed to other Fe-Ti oxides that appear brownish and translucent.

DEVITRIFIED TUFF

Devitrified tuff constitutes the central and most voluminous part of the tuff sheet. Most of it is nonporous and has a density greater than 2.3. Where low in phenocrysts, the tuff is commonly uniform medium

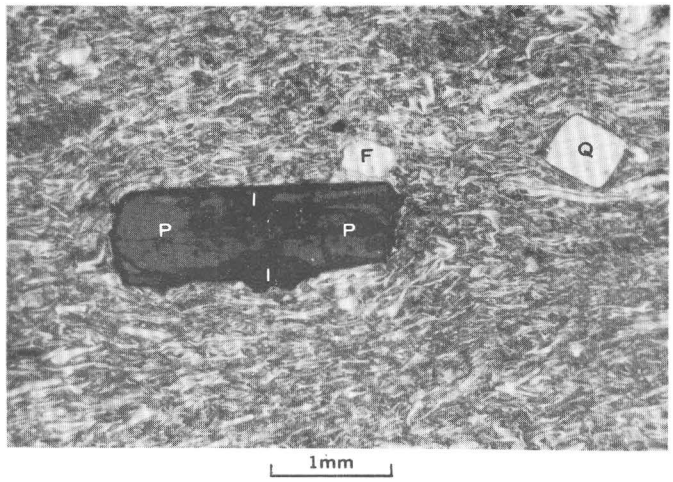

FIGURE 8.—Photomicrograph of tuff from section 154, specimen 1. Moderately dense vitric tuff, shards substantially flattened and stretched. Pyroxene crystal (P) left center, dark margin is relief effect, margin is unaltered; ilmenite inclusions (I) top center and bottom of phenocryst. Alkali feldspar crystal (F) above pyroxene. Euhedral quartz crystal (Q) upper right has typical rhombic outline formed by pyramid faces, showing crystallization as β-quartz. Plain light.

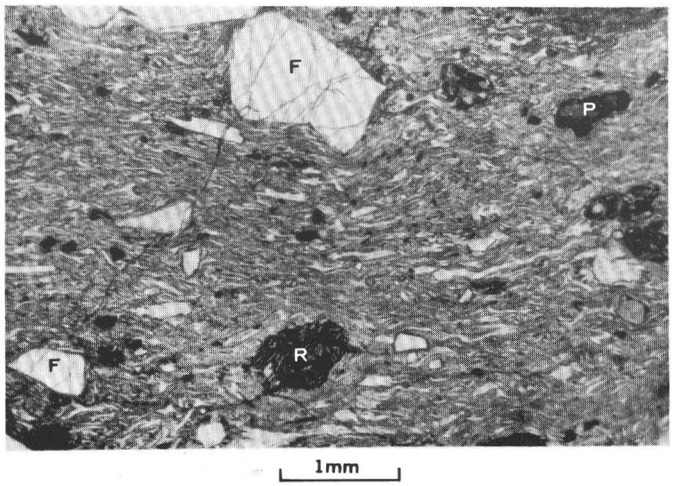

FIGURE 9.—Photomicrograph of tuff from specimen 144. Dense, compact vitric tuff with flattened and stretched shards (colorless) and uniform, pale-brown glass matrix. Alkali feldspar phenocrysts (F) (white) rounded and fractured. Rock fragment (R) in bottom center is andesite; plagioclase phenocrysts visible against dark groundmass. Pyroxene crystal (P) in upper right. Plain light.

gray (*N*–5) to light brownish gray (5 *YR* 6/1), tough and coherent, and weathers only to large blocks (figs. 11, 12). Where richer in phenocrysts the rock is commonly streaked and mottled medium to light gray (*N*5–*N*7) with pinkish, yellowish, and greenish gray (5 *YR* 8/1, 5*Y* 8/1, 5*GY* 6/1). Such tuffs tend to disintegrate to hackly bits upon moderate weathering (fig. 13). Devitrified tuff with density less than 2.3 is visibly porous, commonly light to very light gray (*N*7–8) or yellowish gray (5*Y* 8/1), and quite coherent; it characteristically weathers into large blocks.

The groundmass is a fine aggregate of light minerals with interstitial dark material. Where finest grained, it is dark brown and nearly opaque (fig. 15); where somewhat coarser, it is mottled light and dark browns. Shard structure is clearly evident in some samples (fig. 14) and faint (fig. 15) to obliterated (figs. 16, 17) in others, consisting only of faint parallel streaks around the corners of phenocrysts (fig. 16). Where shards are clearly defined, devitrification products are alined in parallel or spherulitic texture.

Devitrification has affected pumice and phenocrysts in varying degree. Voids lined with a few crystals mark the position of completely collapsed pumice. Relatively coarse, light-colored aggregates also suggest relict pumice fragments. Feldspar and quartz phenocrysts are much like those in the vitric tuff. Pyroxene, magnetite, and ilmenite tend to be more decomposed and rimmed with dark-brown material. Rock fragments, recognizable as andesite in vitric tuff, are mostly dark and indeterminate in samples of devitrified tuff.

LATERAL AND VERTICAL VARIATIONS

MEASURED SECTIONS

The welded tuff of Devine Canyon varies both laterally and vertically in density, phenocryst content, pumice content, and degree of devitrification. Data from 28 measured sections, and from additional localities near the margins of the tuff sheet, provide the basis for the major conclusions concerning these variations. The locations of the sections are shown in figures 3 and 22, and the data for the sections, including thickness, devitrification, modes, and reciprocal density, are summarized in figures 18–21.

At most of the measured sections, actual contacts with underlying units were not observed because these units are soft sediments and do not form good outcrops. However, the presence of vitric welded tuff, locally of lower density, in the lower parts of most sections suggests proximity to the base of the unit. Sections in which vitric bases are not exposed are mostly the thickest ones, located in the area north of Burns. These may indeed be somewhat thicker than shown in the diagrams and may show changes such as decrease in phenocrysts at their true bases; however, the discrepancy would not significantly affect the volume computations.

The tops of most sections occur either at rims, where there are no overlying formations, or at covered intervals, above which is basalt or younger welded tuff. In some sections decreasing density or increasing pumice content at the top suggests proximity to the top of the ash flow. Little pumiceous or ashy sediment rich in

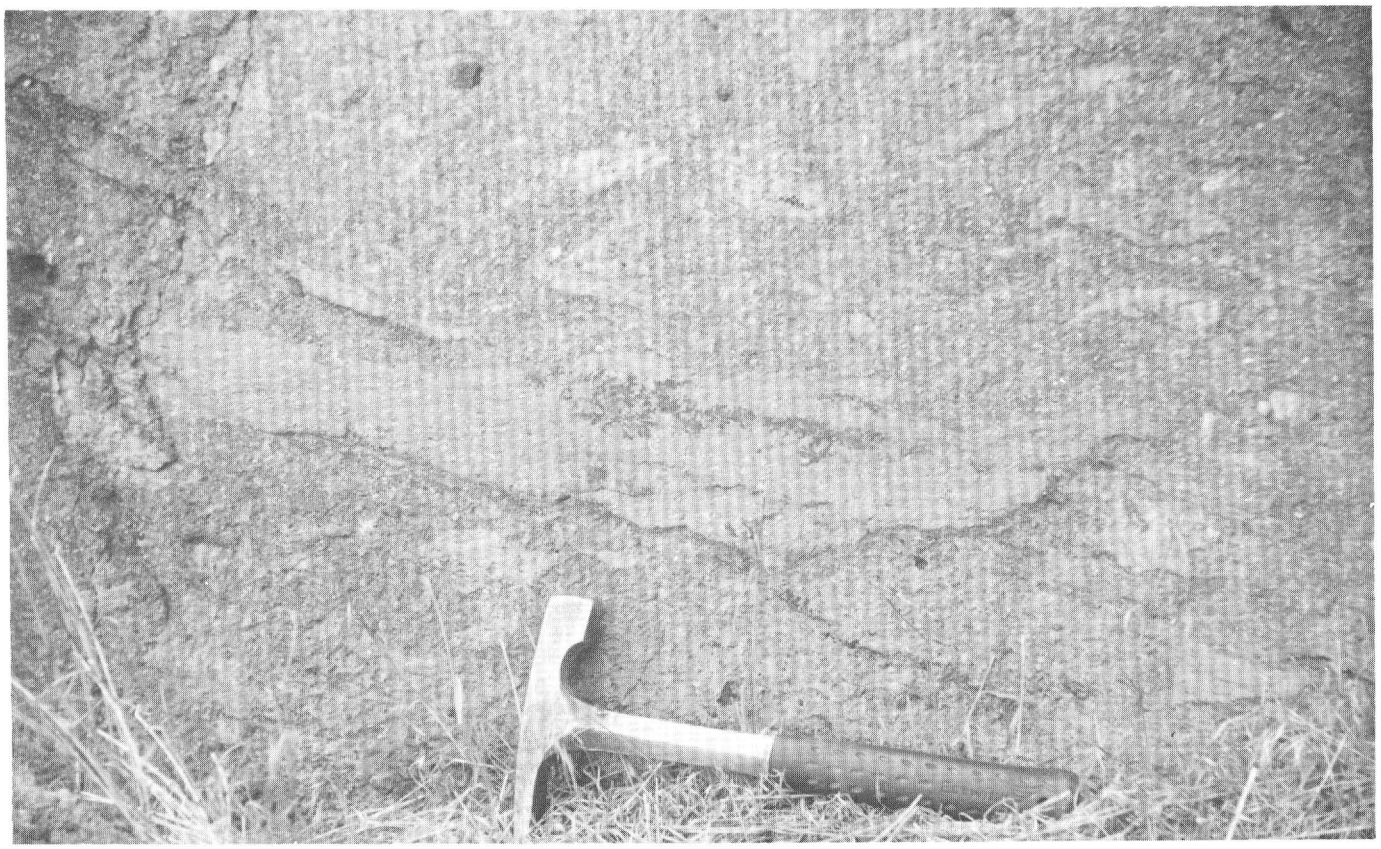

FIGURE 10.—Basal part of Poison Creek section, No. 158 (figs. 12, 19). Length of hammer 11 inches, head 1 inch wide. Abundant pumice lumps 2–3 inches long, longest lump about 20 inches. Abundant phenocrysts of alkali feldspar and quartz distributed throughout both pumice and groundmass.

alkali feldspar crystals appears in sediments younger than the welded tuff of Devine Canyon. Probably no more than a few feet of poorly welded ash-flow tuff has been excluded at the tops of measured sections.

DEVITRIFICATION

At most sections devitrified tuff overlies a relatively thin basal zone of vitric tuff with sharp contact, commonly represented by a notched or cavernous zone in the outcrop (fig. 11). Locally, however, as at the Poison Creek section (fig. 12; sec. 158, fig. 19), there is a transition zone of partly devitrified tuff. At a few sections (for example, secs. 110 and 164, fig. 18) vitric zones overlie a devitrified part.

All sections less than 25 feet thick, and some up to 35 feet thick, consist entirely of vitric tuff (figs. 18–21). A few sections between 25 and 35 feet thick are partly devitrified; this fact suggests that the ash-flow material that accumulated at these places was either hotter or richer in volatiles than that of the sections which remained entirely vitric (Smith, 1960a).

DENSITY

Density values have been determined for specimens from measured sections, and the reciprocal density (a measure of the degree of inflation, or percent pore space in the tuff) is plotted in figures 18–21 to the left of the bar representing the groundmass. The typical pattern of density variation is from low density at the base of a section, to higher density in the middle, to decreased density at the top. Some sections, however, have a fairly uniform high density throughout or have decreased density at the top or base (not both), with various minor fluctuations. All sections probably have at least a narrow zone of tuff of low density at both top and base that would show in the measured sections if exposure were perfect.

Low density near the base implies cooling and welding beyond the point of possible further compaction before the deposition of much overlying tuff. This cooling and welding in turn suggests either multiple flow emplacement or very rapid cooling near the base. Tuff near the top is less dense because there was less overburden to compact it and because it was inflated by escaping volatiles.

PHENOCRYSTS

The variation in alkali feldspar and quartz phenocryst content is the outstanding feature of the welded

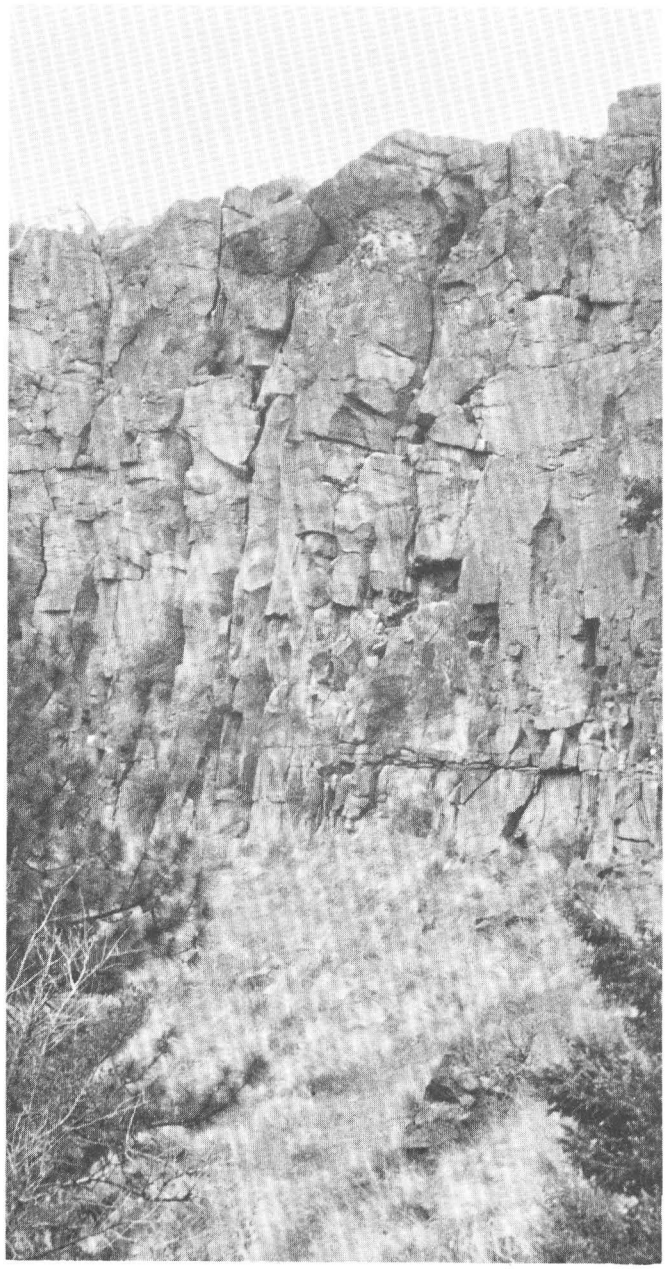

FIGURE 11.—Silvies Canyon section (fig. 19, sec. 160). A typical section, 82 feet thick, showing a composite of features. Small columns in vitric basal part (17 feet), discontinuous parting or notch separates devitrified main part with larger columns formed by more widely spaced joints. Gas cavity zone near top. This section phenocryst-poor from base to top.

tuff of Devine Canyon. Alkali feldspar phenocryst content ranges from about 1 to over 29 percent, generally increasing stratigraphically upward (figs. 18–23). Quartz phenocryst content ranges from 0 to 7 percent and follows much the same pattern as the alkali feldspar variations. The basal few feet of the welded tuff contains less than 10 percent alkali feldspar phenocrysts throughout most of its extent, but it contains much higher percentages in the central area, where the

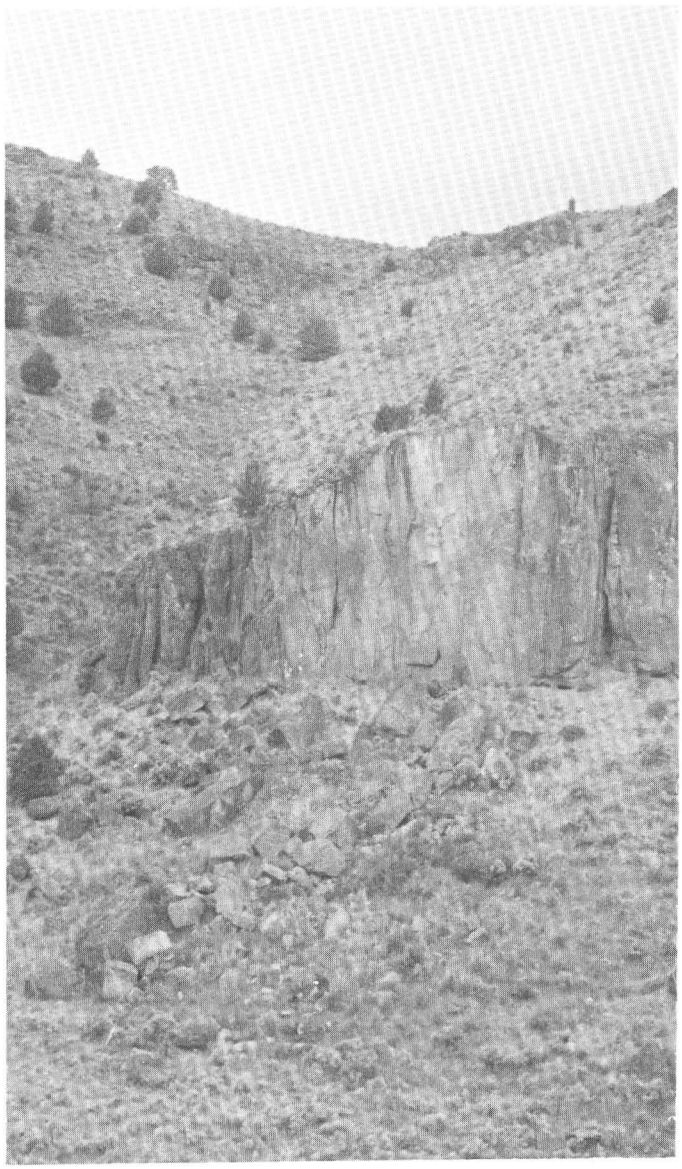

FIGURE 12.—Poison Creek section, reference section for welded tuff of Devine Canyon (fig. 19, sec. 158). Section, 104 feet thick, features even columnar joints from base to top. Transition zone vitric-devitrified tuff not marked by visible change. Crystal and pumice rich at base; both decrease upwards. Weathers to large blocks shown on slope below.

tuff is thickest (fig. 22). Percentages are intermediate in the northwest and northeast. In most sections phenocryst content increases upward from the base, but in some it varies little from base to top (fig. 18, sec. 162; fig. 19, sec. 160; fig. 23, secs. A, B), and in a few it decreases upwards (fig. 19, secs. 9, 158, 159; fig. 23, sec. C), probably because of limited overturn of magma during ascent.

Information from the measured sections and other localities has provided the basis for estimating the volume of the welded tuff with various proportions of alkali feldspar phenocrysts. The volume has been sepa-

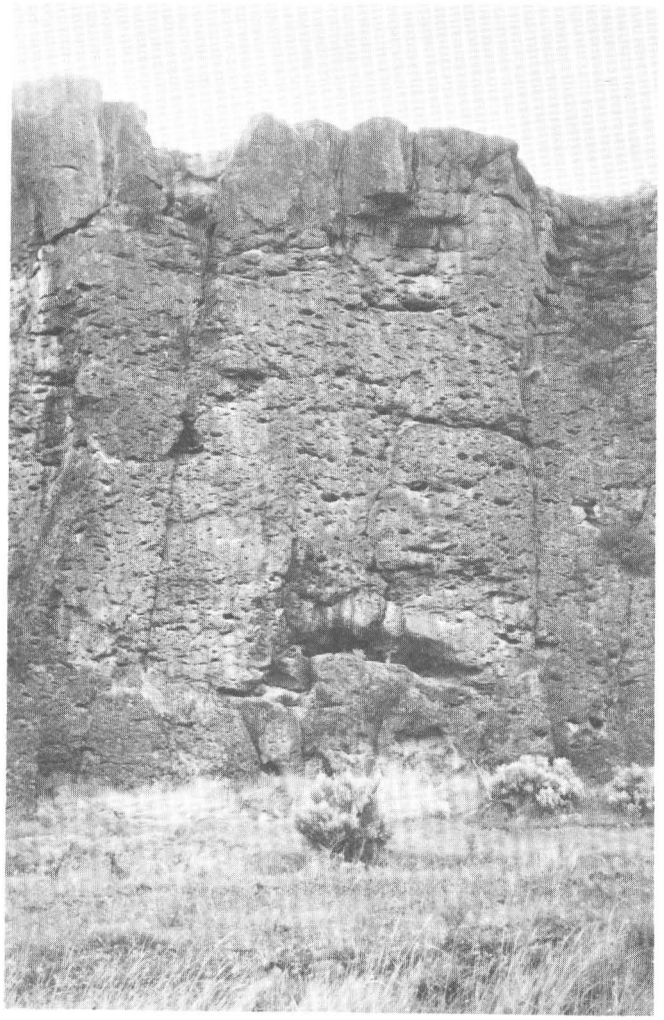

FIGURE 13.—Lower Silvies River section (fig. 19, sec. 159). Section is 85 feet thick. Very widely spaced jointing and abundant gas cavities are features here, tuff is rich in phenocrysts. Base is a flood plain. Silvies River has carried away debris.

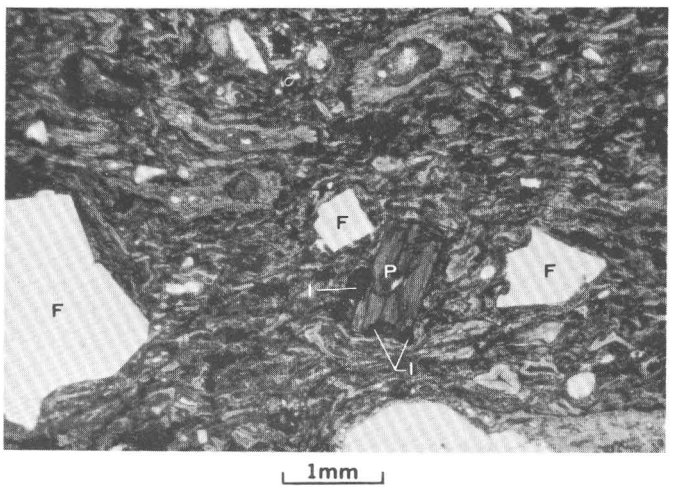

FIGURE 14.—Photomicrograph of tuff from section 160, specimen 3. Devitrified tuff with well-developed flattened shards. Pyroxene crystal (P) right center with ilmenite crystals (I) at margin, light phenocrysts are alkali feldspar (F), stretched pumice lumps in top portion. Plain light.

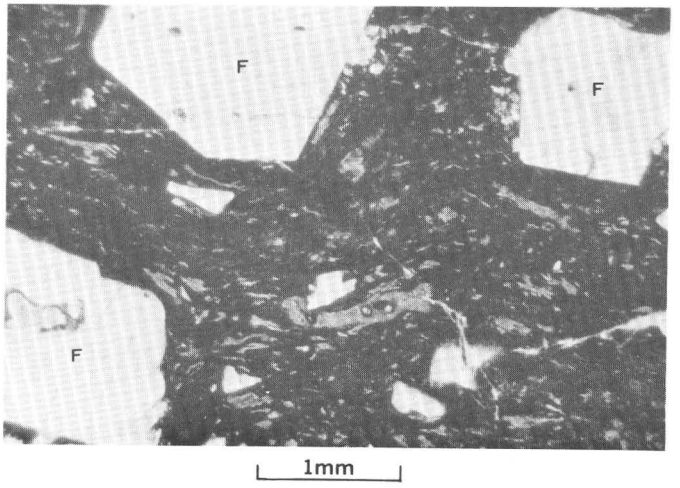

FIGURE 15.—Photomicrograph of tuff from section 163, specimen 3. Devitrified shards and pumice show only as faint, scattered residuals in groundmass. Phenocrysts are alkali feldspar (F); the larger ones euhedral, the smaller ones broken fragments. Plain light.

rately calculated for 0–5, 6–10, 11–15, 16–20, 21–25 and over 25 percent phenocrysts (fig. 24). The results reveal that, unlike more highly differentiated tuffs, such as those in southern Nevada (Lipman and others, 1966; Lipman and Christiansen, 1964; and others), a relatively high proportion of the welded tuff of Devine Canyon is rich in phenocrysts. This is believed to be owing to relatively rapid growth of phenocrysts and eruption of the magma, as discussed later.

PUMICE

Pumice content varies irregularly. In the more densely welded devitrified tuffs, pumice has commonly collapsed and has been reduced to mere streaks in the groundmass. Pumice contents are highest in the lower parts of sections in the central thickest and most crystal-rich part of the tuff. Two sections in the northern and several in the south-central part of the tuff sheet have high pumice contents. In general, pumice content decreases towards the margins of the sheet, suggesting that it was winnowed out of the advancing ash flow before the ash reached its maximum extent (Fisher, 1966).

SOURCE

Regional evidence does not point directly to a source area for the welded tuff of Devine Canyon, nor does it provide much indication of the shape or depth of the magma chamber. The isopach map (fig. 3) shows that the thickest part of the tuff is in the west-central part of the sheet, near Burns, which is at the northwest

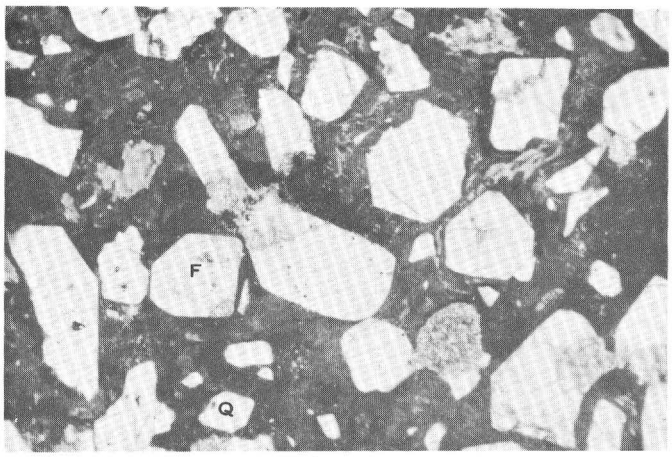

FIGURE 16.—Photomicrograph of tuff from section 9, specimen 1. Abundant phenocrysts, mostly alkali feldspar (F), some quartz (Q); some euhedral, some rounded and embayed, some fragments. Very fine dark devitrified groundmass partially recrystallized (lighter parts). A few light streaky areas are pumice residuals. Plain light.

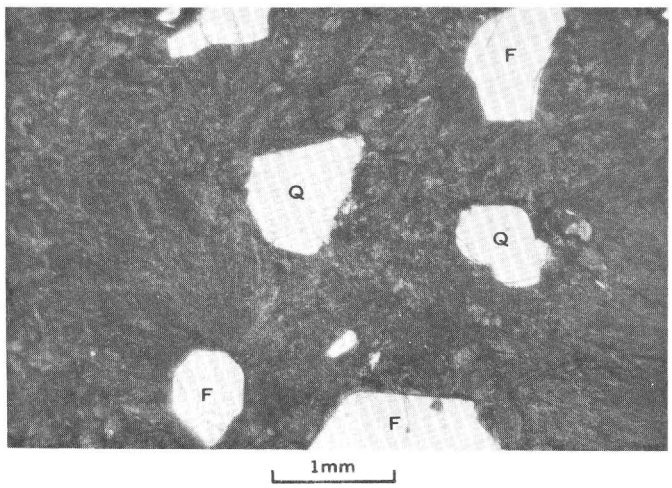

FIGURE 17.—Photomicrograph of tuff from section 158, specimen 3. Quartz phenocrysts (Q), left and right center, alkali feldspar (F) top and bottom. Devitrified groundmass has recrystallized to quartz and alkali feldspar with feathery texture, obliterating all vestiges of shard structure. Plain light.

corner of the Harney Basin lowland (fig. 1). Regional mapping (Piper and others, 1939; Greene and others, 1972; Greene, 1972) has shown the Harney Basin Lowland to be a downwarped and downfaulted area. In particular, the sequence of Pliocene welded tuffs and sediments, including the Devine Canyon, Prater Creek, and Double O Ranch (table 1), dips southerly on the north side of the Harney Basin lowland and is covered by Quaternary sediments at the margin of the lowland. Thus, the source area is probably buried and cannot be exactly located. However, because the tuff is thickest and richest in crystals north of Burns, the most likely source area is considered to lie in the lowland immediately to the south, as indicated in figures 1 and 3.

Downwarping of the Harney Basin Lowland may be in part related to the expulsion of large volumes of magma from beneath. The welded tuffs of Devine Canyon, Prater Creek, and Double O Ranch probably amount to over 100 cubic miles in total volume and all may have come from beneath the lowland. The fact that the lowland is such a large downwarped area (about 1,000 sq mi) and no smaller collapse features have been identified, suggests that the magma bodies that erupted to form these tuffs were most likely of broad, discoidal shape rather than thick cylinders.

PETROLOGY

MINERALOGY

The microscopic appearance of vitric and devitrified groundmass in specimens of this tuff has already been described. X-ray patterns show groundmass minerals in devitrified tuff to be alkali feldspar, cristobalite, quartz, and, more rarely, tridymite. Alkali feldspar is ubiquitous and may be accompanied by one, two, or all three of the silica minerals. In the finest grained, irresolvable groundmass, cristobalite is found (fig. 15); where any bladed, spherulitic, or axiolitic textures appear, quartz is present (fig. 17). Tridymite appears as spongy masses lining small cavities.

Alkali feldspar.—Alkali feldspar phenocrysts are present in all of the tuff and are its most distinctive feature. Amounts range from less than 1 (fig. 6) to 29 percent (fig. 16). In each thin section there are a few euhedral grains showing (100), (010), (001), (110), (101), a majority of grains with some faces and some rounded and embayed surfaces, and some broken fragments (fig. 6–9, 14–17). Carlsbad twins are rare, but almost all grains show faint grid twinning near extinction. Refractive indices, determined on several grains from sample GWW–140–61 (Catlow Valley, near southern limit of tuff sheet), using the spindle stage, are α1.523–4, β1.528–9, γ1.529–30. The 2V's on grains from the same sample ranged from 34° to 37° (−). Chemical analyses of two samples (table 3) show that both have a composition close to $Or_{42}Ab_{57}An_{0.6}$. Feldspar of this composition and high-temperature origin is generally termed sanidine. The monoclinic-triclinic field boundary is placed at $Or_{37}Ab_{63}$; the more potassic monoclinic feldspars are called sanidine and the more sodic triclinic feldspars, anorthoclase (Smith and MacKenzie, 1958, p. 874).

Quartz.—Quartz phenocrysts, like alkali feldspar, are ubiquitous. They range in amount from less than 1 to 7 percent. As seen in thin section, they are euhedral, rounded and embayed, or angular fragments. Euhedral crystals commonly show prism faces doubly terminated

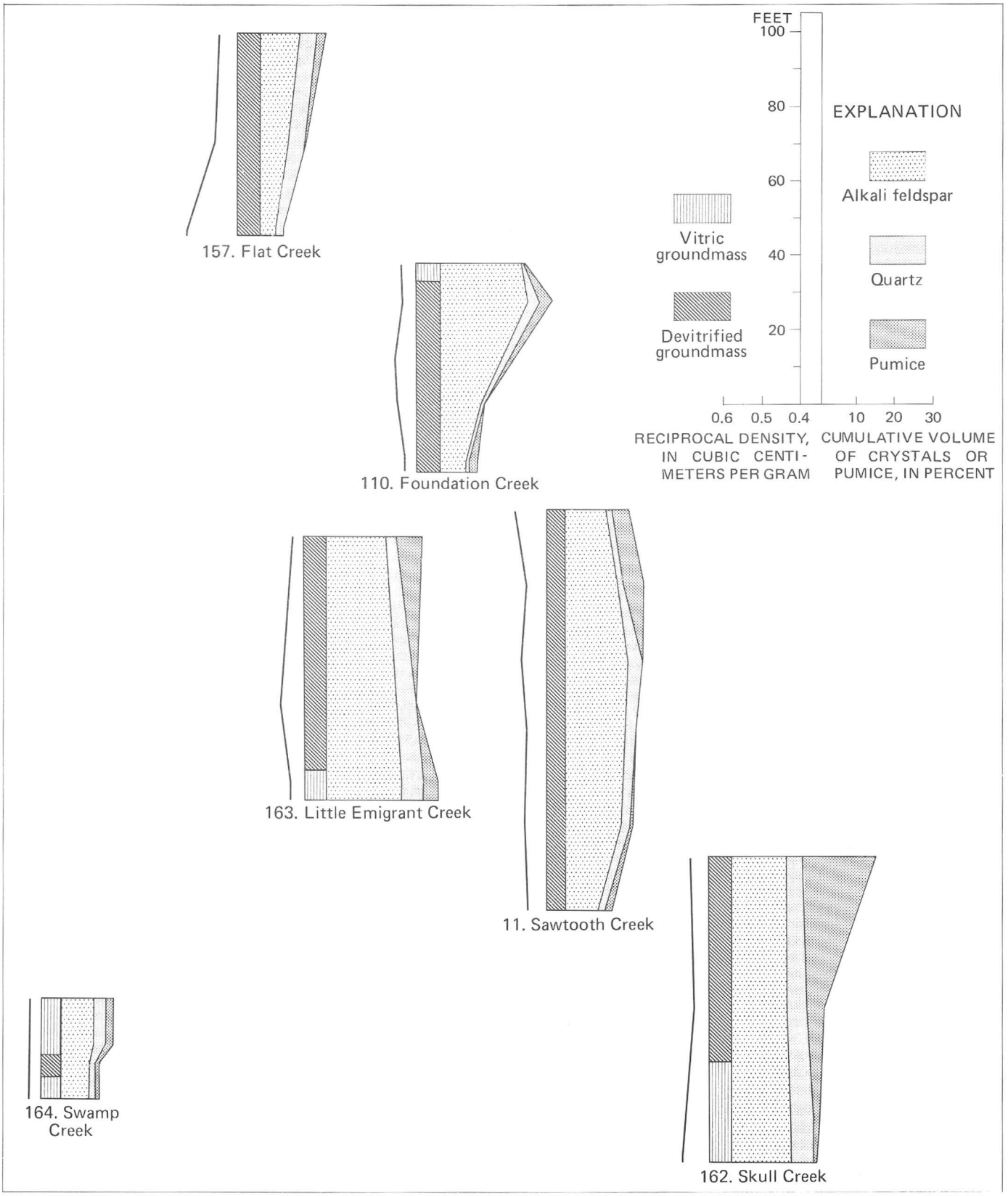

FIGURE 18.—Measured sections of welded tuff of Devine Canyon, northwestern part. Central bar of each diagram shows thickness of section and devitrification of groundmass. Line to left indicates reciprocal density; patterns to right, cumulative volume percent of crystals or pumice.

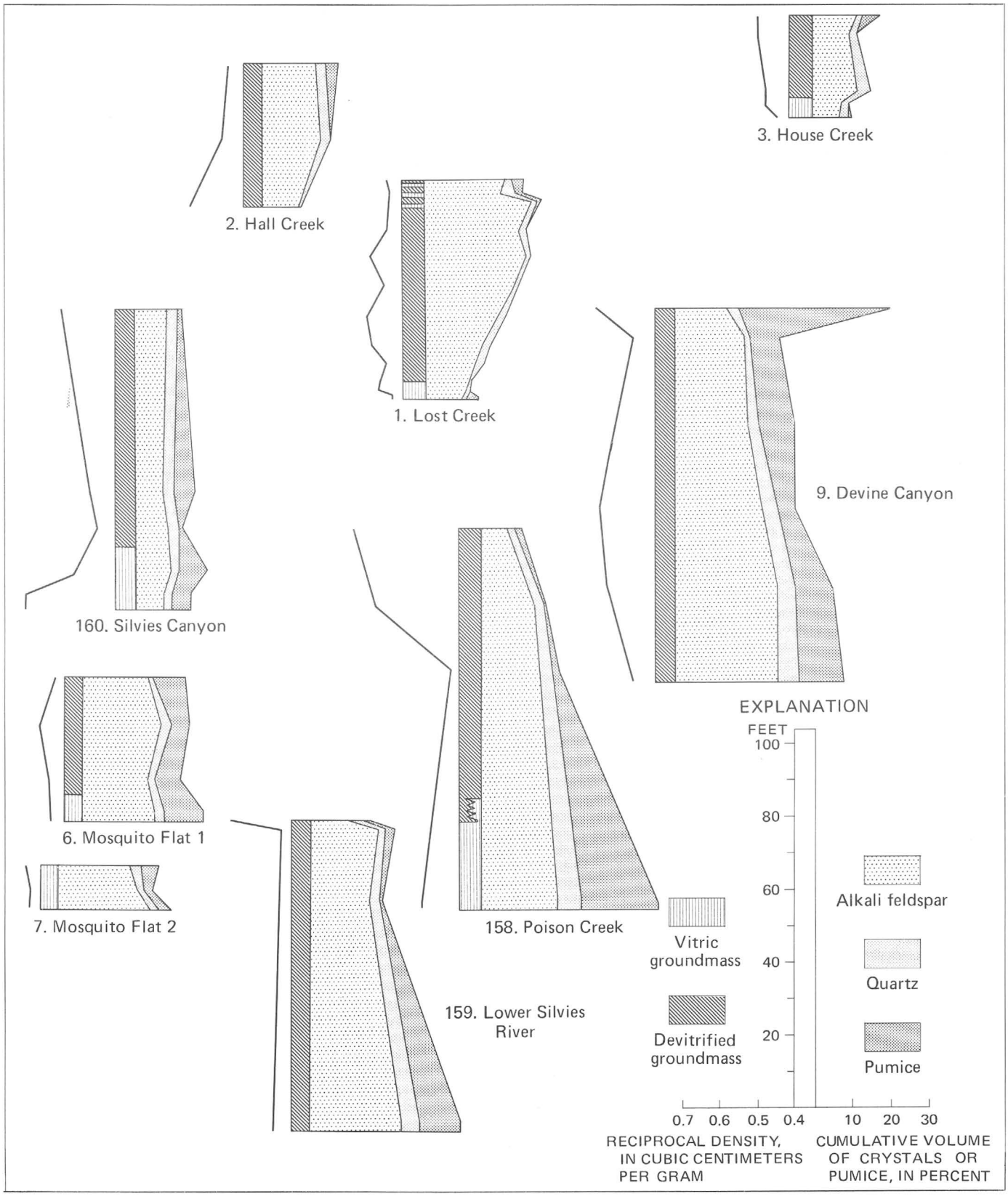

FIGURE 19.—Measured sections of welded tuff of Devine Canyon, north-central part. Central bar of each diagram shows thickness of section and devitrification of groundmass. Line to left indicates reciprocal density; patterns to right, cumulative volume percent of crystals or pumice.

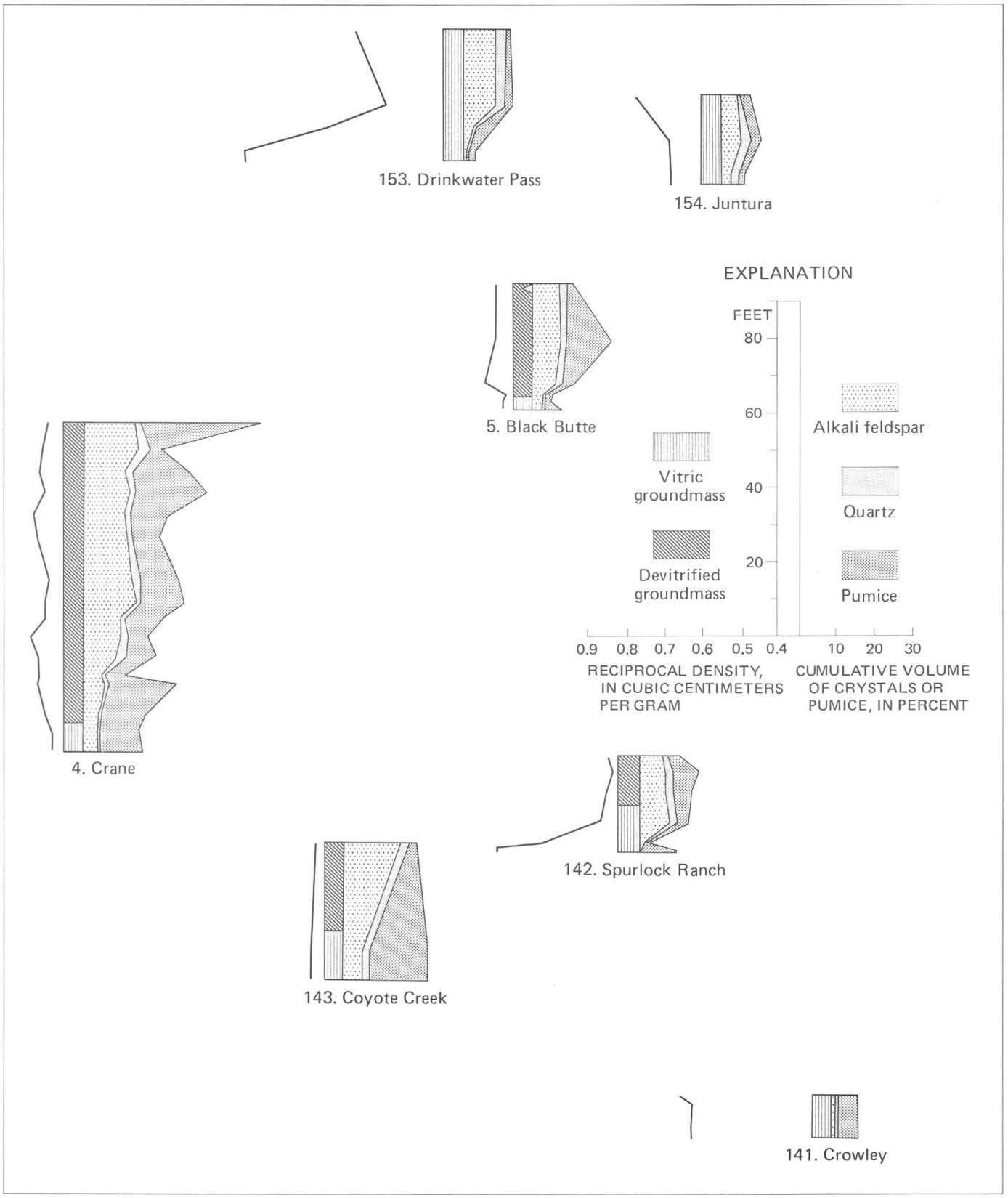

FIGURE 20.—Measured sections of welded tuff of Devine Canyon, eastern part. Central bar of each diagram shows thickness of section and devitrification of groundmass. Line to left indicates reciprocal density; patterns to right, cumulative volume percent of crystals or pumice.

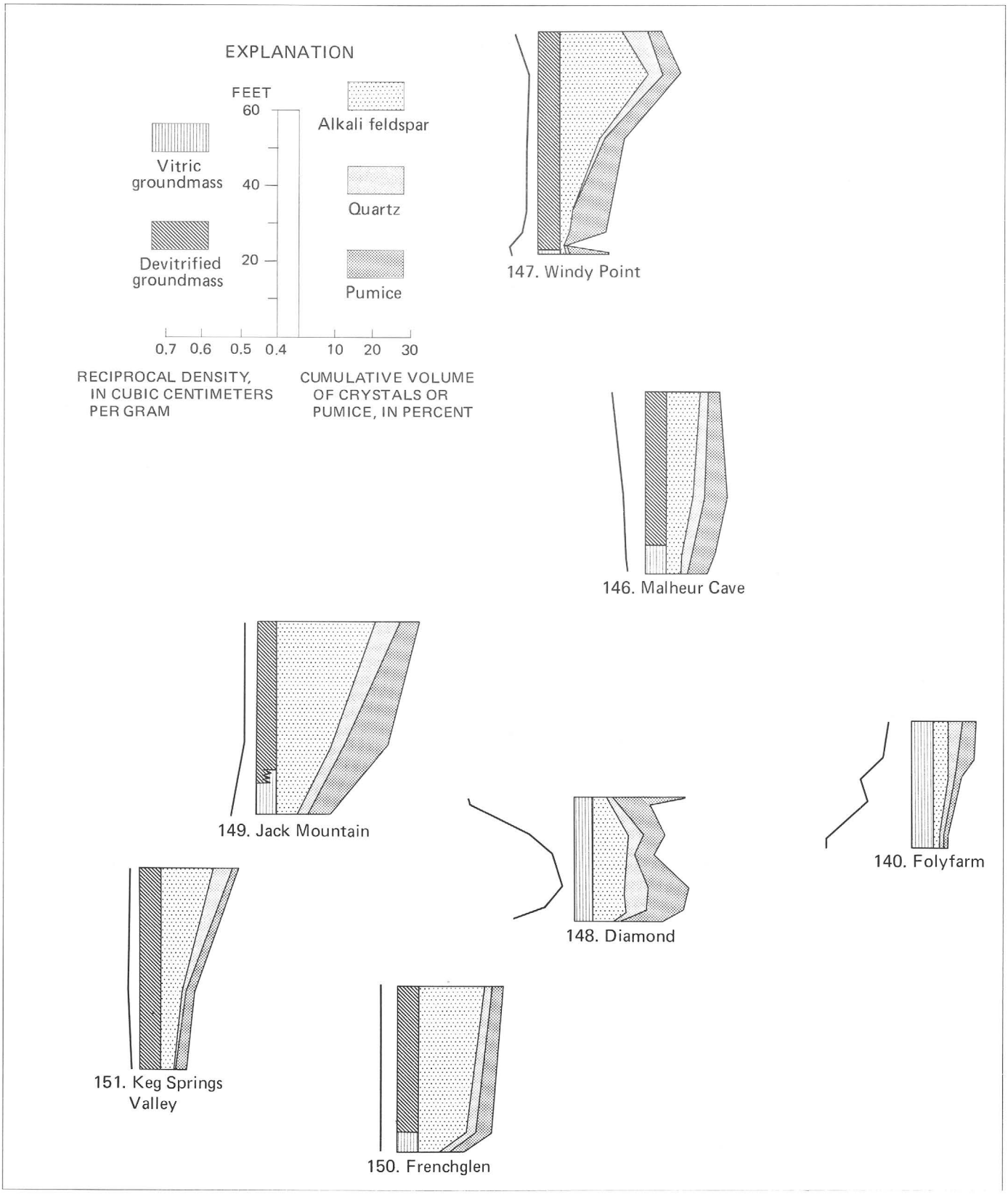

FIGURE 21.—Measured sections of welded tuff of Devine Canyon, southern part. Central bar of each diagram shows thickness of section and devitrification of groundmass. Line to left indicates reciprocal density; patterns to right, cumulative volume percent of crystals or pumice.

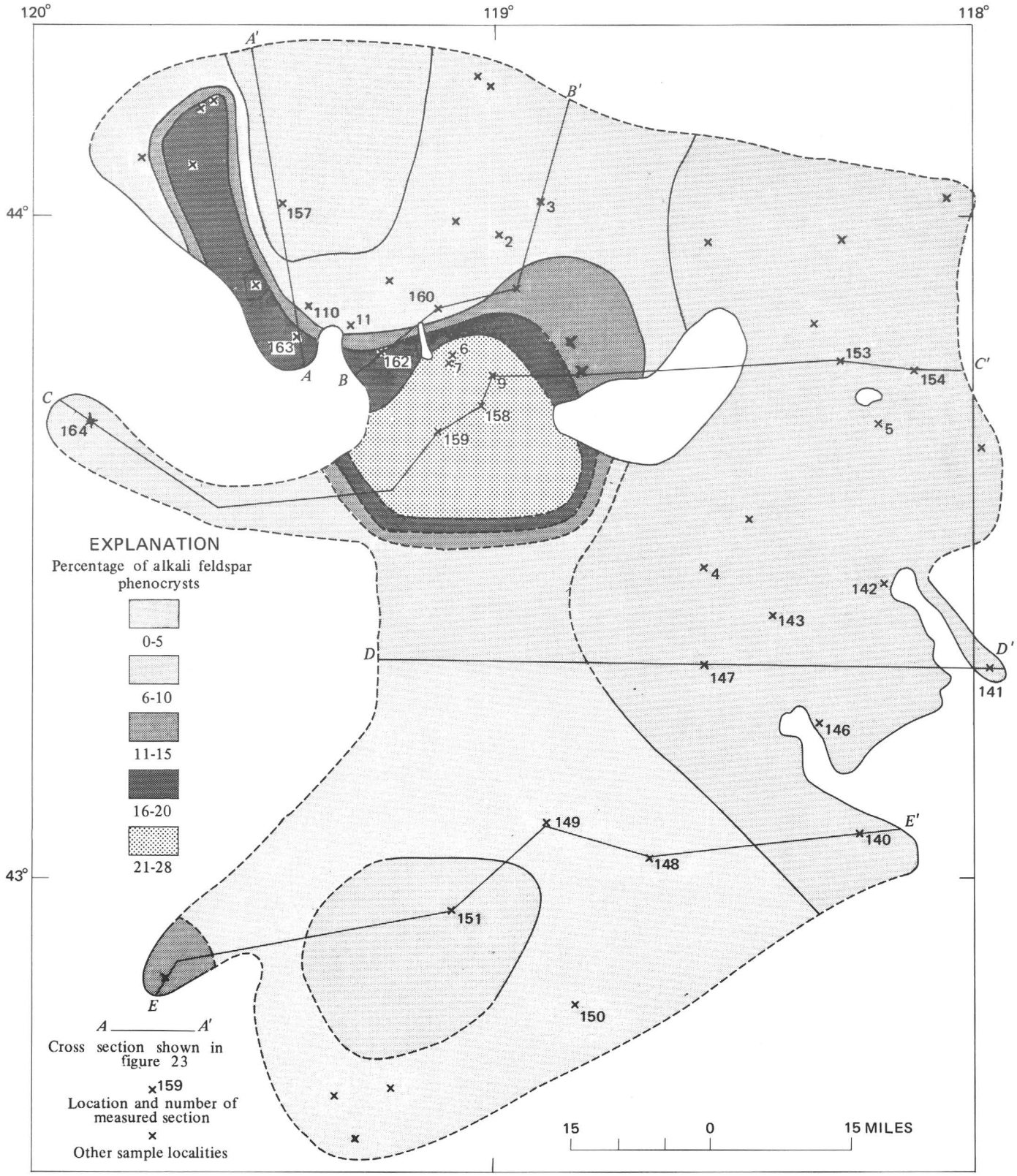

FIGURE 22.—Alkali feldspar phenocrysts in basal few feet of tuff sheet.

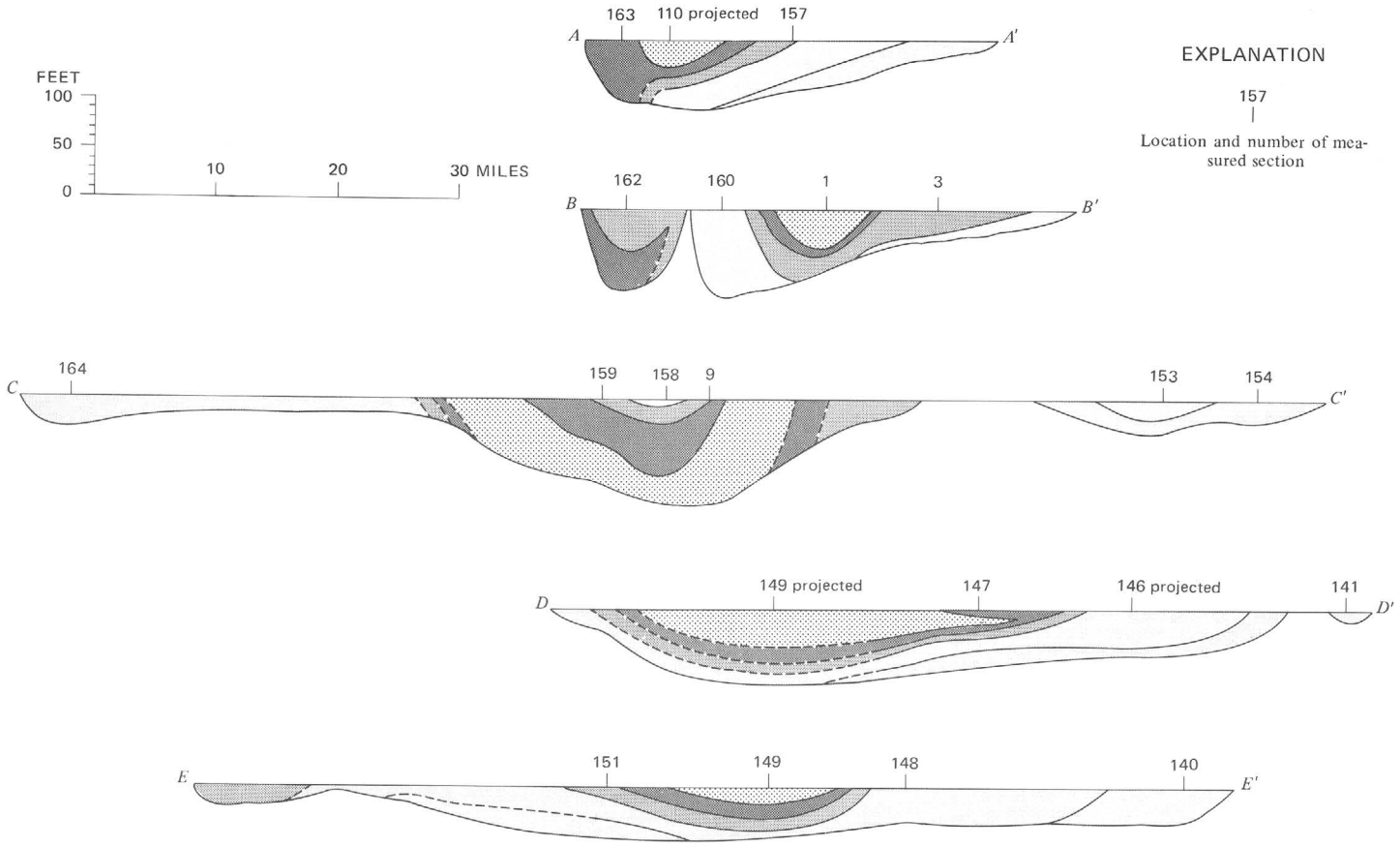

FIGURE 23.—Cross section illustrating variations in alkali feldspar phenocryst content. (See fig. 22.)

TABLE 3.—*Analyses of alkali feldspar phenocrysts from the welded tuff of Devine Canyon*

[Partial chemical analyses for SiO_2, Al_2O_3, Fe_2O_3, CaO, Na_2O, and K_2O, by Lois M. Jones and Lois B. Schlocker. Quantitative spectrographic analyses for Sr and Ba by R. E. Mays. Quantitative spectrographic analyses for Li, Cs, and Rb by Harry Bastron]

	WT-6 Windy Point	140-61 Catlow Valley
SiO_2	67.5	67.5
Al_2O_3	18.4	18.5
Fe_2O_3[1]	.47	.36
CaO	.11	.13
Na_2O	6.2	6.2
K_2O	7.0	6.8
Sr	.0026	.0040
Ba	.016	.022
Li	.0002	.0003
Rb	.004	.004
Normative values:		
An	.55	.67
Ab	57.1	57.8
Or	42.4	41.7

[1]Total iron expressed as Fe_2O_3. Cs not detected.

by pyramid faces at the ends, suggesting crystallization as beta-quartz (fig. 8, pyramid faces only).

Clinopyroxene.—Sparse clinopyroxene phenocrysts are visible in about two-thirds of the thin sections studied and are probably sparsely distributed throughout the tuff. The tiny crystals can rarely be seen in hand specimen. In thin section, the clinopyroxene is pleochroic from dark to pale green where fresh, or pale green to colorless where altered. Some crystals are rimmed with a dark to opaque margin, probably owing to oxidation during eruption. Characteristic pyroxene cleavage is visible, and faces of the forms (100), (101), ($\bar{1}$01) (fig. 8), (010), and (110). Refractive indices and optic angles (table 4) indicate compositions of $Wo_{27}En_4Fs_{69}$ and $Wo_{38}Fs_{62}$ for two samples (Hess, 1949). X-ray single crystal and powder data for one sample (table 5) indicate a composition of $Wo_{42}En_8Fs_{50}$ (Brown, 1960). The high refractive indices are responsible for the higher Fs content indicated by the optical data. However, all determinations fall in the ferrohedenbergite field according to Poldervaart and Hess' nomenclature (1949).

BULK COMPOSITION

ANALYSES

Analyses of 14 samples of the welded tuff of Devine Canyon (table 6) indicate that in terms of composition

TABLE 4.—*Optical properties of pyroxene from welded tuff of Devine Canyon*

Sample	148-3	163-1	162-2
α	1.726–32	1.731–5	.....
β	1.743–7	1.740–5	1.744–8
γ	1.762–5	1.761	.....
2V	53°–54°	.....	61°–62°

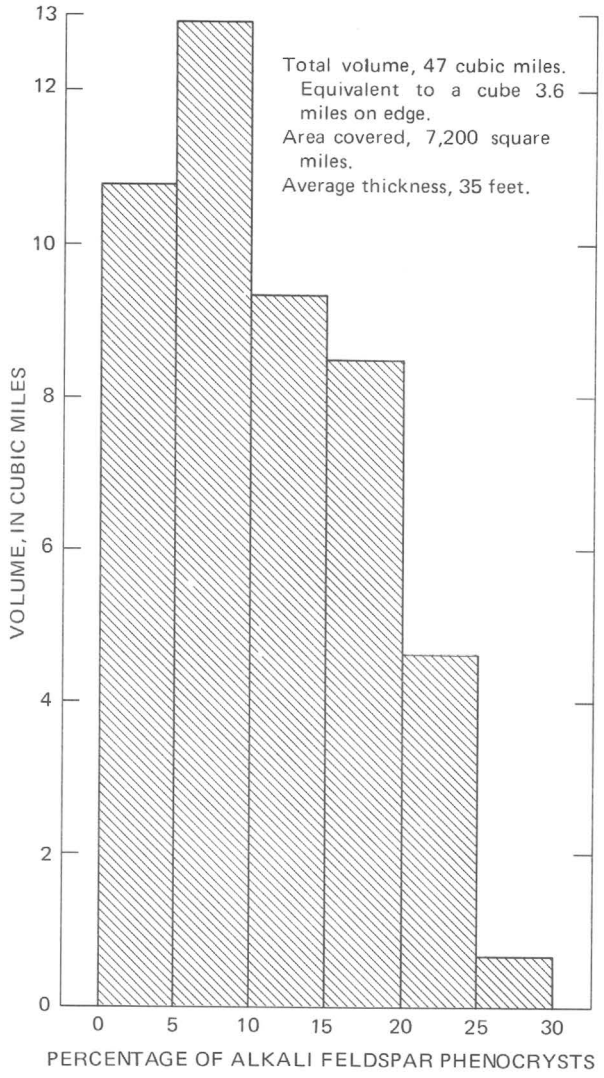

FIGURE 24.—Histogram showing relative volumes of tuff with various phenocryst contents.

the vitric and devitrified tuffs each from a rather homogeneous group. Vitric tuff has less Na_2O, less SiO_2, more K_2O, and more H_2O^+ than devitrified tuff, probably as a result of selective leaching of Na from the vitric tuff by ground water (Lipman, 1965). Na is replaced by K. Water remains in the structure, its added weight causing a decrease in the weight percent of the most abundant component, SiO_2. Slight increase of Al_2O_3 in the vitric tuffs, as suggested by Lipman, is not borne out by these data; iron is generally less oxidized.

Inasmuch as there is no nonhydrated glass, the devitrified tuffs best represent magmatic compositions (Lipman and others, 1969). Since the Na_2O contents of these tuffs range from 3.7 to 4.3 percent (table 6), they are unlikely to have lost Na during crystallization as did the comendite tuffs, with initial Na contents over 5 percent, that Noble (1970b) described. Compositions

TABLE 5.—*X-ray diffraction data for pyroxene from sample 148–3*

[Analyses by R. C. Erd. Chart X3417, ilmenite peaks abstracted; Cu/Ni, Si internal standard; ¼°, ¼"/minute]

Calculated		Measured		Calculated		Measured	
hkl	d (A) *hkl*	d (A) *hkl*	I	*hkl*	d (A) *hkl*	d (A) *hkl*	I
110	6.531	6.524	88	112	2.216		
200	4.735	4.735	36	$\bar{2}22$	2.202		
020	4.509	4.507	10	022	2.199		
$\bar{1}11$	4.404			330	2.177	2.176	26
111	3.672			$\bar{3}31$	2.149	2.147	22
021	3.360	3.358	4	$\bar{4}21$	2.123	2.120	16
220	3.266	3.265	58	420	2.096		
$\bar{2}21$	3.007	3.008	66	041	2.058	2.058	4
310	2.980	2.979	100	240	2.036		
$\bar{3}11$	2.909	2.905	14	$\bar{4}02$	2.017	2.017	8
130	2.865			202	2.010		
$\bar{1}31$	2.583	2.584	14	$\bar{1}32$	1.973		
221	2.534	2.534	28	$\bar{2}41$	1.968		
$\bar{2}02$	2.523			$\bar{5}11$	1.910		
002	2.518			331	1.876		
$\bar{1}12$	2.512			510	1.854	1.854	6
131	2.408			$\bar{4}22$	1.841		
400	2.368	2.367	4	222	1.836		
311	2.319					1.772	22
040	2.255	2.254	1			1.637	36
$\bar{3}12$	2.222					1.633	36
						1.579	10
						1.566	18
						1.536	8
						1.503	10
						1.468	3
						1.418	6

A. Precession data:
C z/c — a (A) = 9.830; b = 9.014; c = 5.250; β = 105°34′

B. X-ray powder data: (least squares refinement)
a (A) = 9.834±0.002
b = 9.018±0.001
c = 5.320±0.004
β = 105°37′±2′
Vol. (A^3) = 446.7±0.3
$a:b:c$ = 1.090:1:0.5800
$a \sin \beta$ = 9.470A

C. X-ray fluorescence shows (pyroxene+ilmenite)
Major Fe>>Ca
Minor Ti>Mn

D. d-spacings of associated ilmenite (chart X3417) indicate near end member ilmenite (Berry and Thompson, 1962, p. 175; Deer, Howie, and Zussman, 1962, p. 31).

E. Crystal chosen had forms [100], [010], [110]

F. Compare with data for augite from Kahanui, New Zealand (Clark and others, 1969, p. 34, table 2); also note large cell volume.

G. Diagram of Brown (in Deer and others, 1962, p. 111) gives Wo_{42} En_8 Fs_{50} from powder data, and Wo_{43} En_{10} Fs_{47} from precession value for b.

of the devitrified tuff form a closely knit group that fall partly in the soda rhyolite field and partly in the alkali rhyolite field on Rittman's diagrams (1952).

Semiquantitative spectrographic analyses (table 7) reveal only minor fluctuations in trace elements from sample to sample, except that some samples relatively rich in calcium are also high in strontium and barium.

NORMS

Computer-calculated CIPW norms of the 14 analyzed samples (table 8) show that quartz, orthoclase, and albite are the major normative components. Proportions of orthoclase and albite vary between vitric and devitrified samples, as do the K_2O and Na_2O contents, although further complications, such as Al_2O_3 content, affect these normative components in some samples.

In eight samples there is insufficient Al_2O_3 to use up all the Na_2O in albite, and the excess Na_2O appears as

TABLE 6.—*Rapid rock analyses of vitric and devitrified welded tuff of Devine Canyon*

[Samples 147–1, 160–1, 154–1, 147–3, 151–2, and 160–4 analyzed by P. Elmore, G. Chloe, J. Kelsey, S. Botts, H. Smith, L. Artis, and J. Glenn by method described by Shapiro (1967). Other samples analyzed by P. Elmore, H. Smith, G. Chloe, J. Kelsey, and J. Glenn by method described by Shapiro and Brannock (1962), supplemented by atomic absorption]

Sample	147–1	160–1	154–1	147–3	4–7	4–12	4–16
Section	Windy Point Vitric	Silvies Canyon Vitric	Juntura Vitric	Windy Point Devitrified	Crane Devitrified	Crane Devitrified	Crane Devitrified
SiO_2	73.2	73.8	73.8	75.2	74.1	75.0	75.1
Al_2O_3	10.6	11.4	11.0	10.8	10.9	11.0	11.4
Fe_2O_3	2.6	1.0	2.2	2.8	2.8	3.2	2.5
FeO	.62	.86	.78	.46	.36	.76	.36
MgO	.37	.10	.10	.29	.35	.13	.20
CaO	.44	.24	.30	.25	.69	.30	.42
Na_2O	3.4	3.4	3.0	4.2	4.0	4.0	4.1
K_2O	5.1	5.0	5.6	4.4	4.6	4.5	4.6
H_2O+	2.7	2.5	2.6	.91	.83	.54	.70
H_2O-	.76	.17	.25	.49	.83	.54	.70
TiO_2	.18	.19	.18	.18	.14	.18	.14
P_2O_5	.02	.02	.02	.03	.09	.10	.04
MnO	.04	.03	.04	.04	.06	.07	.06
CO_2	<.05	<.05	<.05	<.05	<.05	<.05	<.05

Sample	151–2	149–3	149–5	160–4	9–1	9–3	9–6
Section	Keg Springs Valley Devitrified	Jack Mountain Devitrified	Jack Mountain Devitrified	Silvies Canyon Devitrified	Devine Canyon Devitrified	Devine Canyon Devitrified	Devine Canyon Devitrified
SiO_2	74.2	75.4	75.3	75.3	75.2	73.6	74.1
Al_2O_3	11.0	11.0	12.0	11.4	11.6	11.2	12.0
Fe_2O_3	3.2	.60	.76	3.0	1.6	2.1	2.2
FeO	.02	.60	.76	.00	1.6	.56	.76
MgO	.31	.10	.10	.18	.13	.83	.24
CaO	.83	.25	.31	.43	.25	.77	.34
Na_2O	4.3	4.0	3.7	4.3	3.7	3.8	4.0
K_2O	4.3	4.5	4.9	4.2	4.4	4.5	4.6
H_2O+	.75	.75	.53	.57	.57	.87	.67
H_2O-	.55	.55	.27	.40	.53	.53	.63
TiO_2	.20	.21	.24	.19	.21	.26	.28
P_2O_5	.06	.08	.06	.04	.03	.06	.06
MnO	.05	.05	.04	.04	.08	.07	.07
CO_2	<.05	<.05	<.05	<.05	<.05	<.08	<.05

acmite. This has no relationship to the mode, as the small amount of clinopyroxene present is nonsodic.

Plots of the normative feldspar components on the lower central part of the An-Or-Ab triangular diagram (fig. 25) reflect the secondary K_2O-Na_2O variations discussed above. The vitric tuffs have more than 50 percent orthoclase, and the devitrified ones have more than 50 percent albite. The reason that a few samples contain normative anorthite is that their Al_2O_3 (not CaO) content is higher than the others. The normative composition of the feldspar from sample GWW–140–61 (table 3) falls among the group of normative feldspar components from devitrified tuffs; this fact suggests that phenocryst feldspar and groundmass feldspar are similar in composition.

The ratios of normative quartz-orthoclase-albite for the devitrified tuffs plot in a loose cluster on the Q-Or-Ab triangle (fig. 26). The fact that Q+Or+Ab totals

TABLE 7.—*Semiquantitative six-step spectrographic analyses of some samples of the welded tuff of Devine Canyon*

[In ppm. N=not detected. Looked for but not detected: Ag, As, Au, Bi, Cd, Co, Ni, Pd, Pt, Sb, Sc, Sn, Te, U, W, Zn, Ge, Hf, In, Li, Re, Ta, Th, Tl, Pr, Sm, Eu, Gd, Tb, Dy, Ho, Er, Tm, Lu. Samples 147–1, 160–1, 154–1, 147–3, 151–2, and 160–4 analyzed by R. E. Mays. Other samples analyzed by Chris Heropoulos]

Sample	147–1	160–1	154–1	147–3	4–7	4–12	4–16
Section	Windy Point Vitric	Silvies Canyon Vitric	Juntura Vitric	Windy Point Devitrified	Crane Devitrified	Crane Devitrified	Crane Devitrified
B	50	50	50	50	50	30	50
Ba	30	70	30	30	150	50	100
Be	7	7	7	7	7	7	7
Cr.	N	N	N	N	1.5	1	1
Cu	15	10	15	15	10	7	7
La	100	70	100	50	150	100	100
Mo	N	N	N	N	N	N	N
Nb	100	100	100	100	50	70	70
Ni	20	20	20	20	N	N	N
Pb	50	50	50	50	30	30	50
Sn	N	N	N	N	N	7	7
Sr	10	7	N	N	30	10	15
V	N	N	N	N	10	7	10
Y	200	150	150	150	150	150	100
Zr	1,500	1,500	1,500	1,500	1,000	1,000	1,000
Ce	N	N	N	N	150	150	150
Ga	30	30	30	30	50	30	30
Yb	20	20	20	20	15	15	15
Nd	N	N	N	N	100	70	100

TABLE 7.—*Semiquantitative six-step spectrographic analyses of some samples of the welded tuff of Devine Canyon*—Continued

Sample	151–2	149–3	149–5	160–4	9–1	9–3	9–6
Section	Keg Springs Valley Devitrified	Jack Mountain Devitrified	Jack Mountain Devitrified	Silvies Canyon Devitrified	Devine Canyon Devitrified	Devine Canyon Devitrified	Devine Canyon Devitrified
B	50	50	20	50	30	30	20
Ba	70	70	200	70	200	300	200
Be	7	5	3	7	5	2	3
Cr	N	1.5	1	N	3	3	3
Cu	20	7	5	15	7	7	7
La	50	100	150	70	150	100	200
Mo	N	5	5	N	N	N	N
Nb	100	50	30	100	30	30	50
Ni	20	N	N	20	N	N	N
Pb	50	20	20	50	30	10	20
Sn	N	N	N	N	N	N	N
Sr	20	15	15	20	15	70	30
V	N	7	7	N	N	10	7
Y	150	150	70	150	100	70	100
Zr	1,500	1,000	700	1,500	700	500	700
Ce	N	200	200	N	200	200	300
Ga	30	30	30	30	30	20	30
Yb	20	15	10	15	10	7	10
Nd	N	100	100	N	150	100	150

TABLE 8.—*Norms of analyzed samples of vitric and devitrified welded tuff of Devine Canyon*

Sample	147–1	160–1	154–1	147–3	4–7	4–12	4–16
Section	Windy Point Vitric	Silvies Canyon Vitric	Juntura Vitric	Windy Point Devitrified	Crane Devitrified	Crane Devitrified	Crane Devitrified
Q	33.5	34.5	34.5	34.3	33.0	34.7	33.4
C	.....	.007	.....	.....	.....	.....	.....
Or	30.1	29.9	33.1	26.0	27.3	26.6	27.2
Ab	26.1	29.1	25.4	31.0	30.6	31.5	33.1
An	.....	1.1	.01	.....	.....	.....	.....
Ac	2.3	.....	.....	3.9	3.0	2.0	1.5
Wo	.87	.....	.56	.39	1.2	.35	.76
En	.92	.25	.23	.72	.88	.32	.50
Fs	.....	.50	.....	.....	.....	.....	.....
Mt	1.6	1.47	1.83	1.1	1.0	2.2	1.0
Hm	.69	.....	.94	.68	1.1	1.0	1.3
Il	.34	.37	.53	.34	.27	.34	.27
Tn	.....	.....	.....	.....	.....	.....	.....
Ap	.47	.05	.05	.07	.21	.23	.10
Q+Ab+Or	89.7	93.5	93.0	91.3	90.9	92.8	93.7

Sample	151–2	149–3	149–5	160–4	9–1	9–3	9–6
Section	Keg Springs Valley Devitrified	Jack Mountain Devitrified	Jack Mountain Devitrified	Silvies Canyon Devitrified	Devine Canyon Devitrified	Devine Canyon Devitrified	Devine Canyon Devitrified
Q	32.4	35.3	34.4	32.9	35.6	32.5	32.3
C	.....	.....	.19	.....	.37	.....	.....
Or	25.5	26.7	29.0	24.8	26.0	26.8	27.2
Ab	32.7	31.7	31.3	35.2	31.3	32.4	33.9
An	.....	.....	1.1	.....	1.0	.2	1.2
Ac	3.3	2.05	.....	2.5	.....	.....	.....
Wo	1.4	.30	.....	.57	.....	1.35	.04
En	.77	.25	.25	.45	.32	2.09	.60
Fs	.....	.....	.....	.....	1.4	.....	.....
Mt	.....	1.5	1.9	.....	2.3	1.3	1.9
Hm	2.1	.3	.4	2.1	.....	1.2	.9
Il	.15	.40	.46	.09	.40	.50	.53
Tn	.30	.....	.....	.36	.....	.....	.....
Ap	.14	.19	.14	.10	.07	.14	.14
Q+Ab+Or	90.6	93.7	94.7	92.9	92.9	91.7	93.4

90 percent or more in each case shows that these points approximate the magma composition.

GROUNDMASS COMPOSITION

Major-element groundmass compositions have been calculated for several of the analyzed devitrified tuffs (table 9). These calculations show that the composition of the groundmass is similar to that of the bulk rock in rocks with few phenocrysts but significantly different in rocks with many. In phenocryst-rich rocks the groundmass contains more SiO_2 and less Al_2O_3, Na_2O, and K_2O than the rock as a whole. This indicates a loss of feldspar components and a corresponding increase in silica in the groundmass (that is, the feldspar-silica mineral ratio is higher in phenocrysts than in the groundmass[1]).

The groundmass compositions of the phenocryst-rich rocks also differ significantly from the average bulk-rock composition (table 9), but the bulk-rock compositions of these same rocks do not differ signifi-

[1]This ratio is between 2 and 20 for phenocrysts from most samples. Feldspar-silica ratio of average whole-rock normative composition is 1.74.

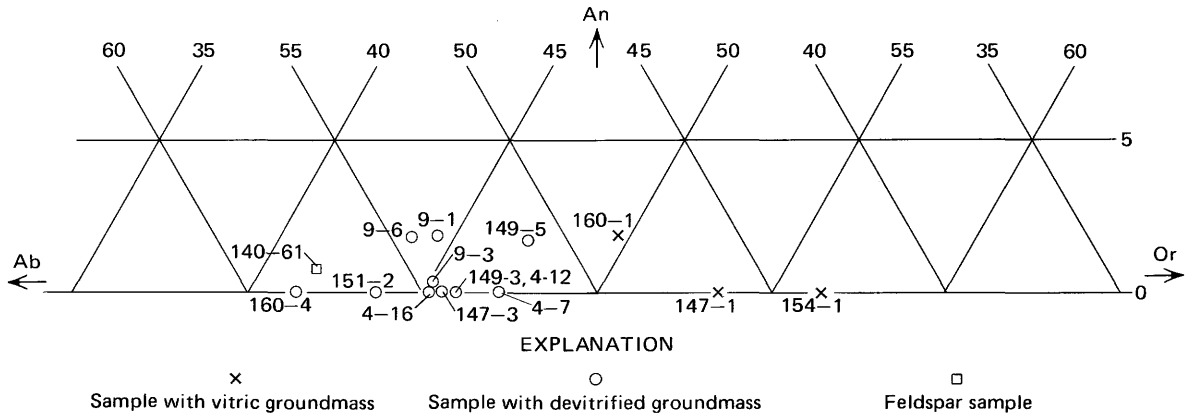

FIGURE 25.—Normative feldspar components of analyzed samples plotted on part of the feldspar triangle. Includes normative components of one analyzed sample of alkali feldspar phenocrysts.

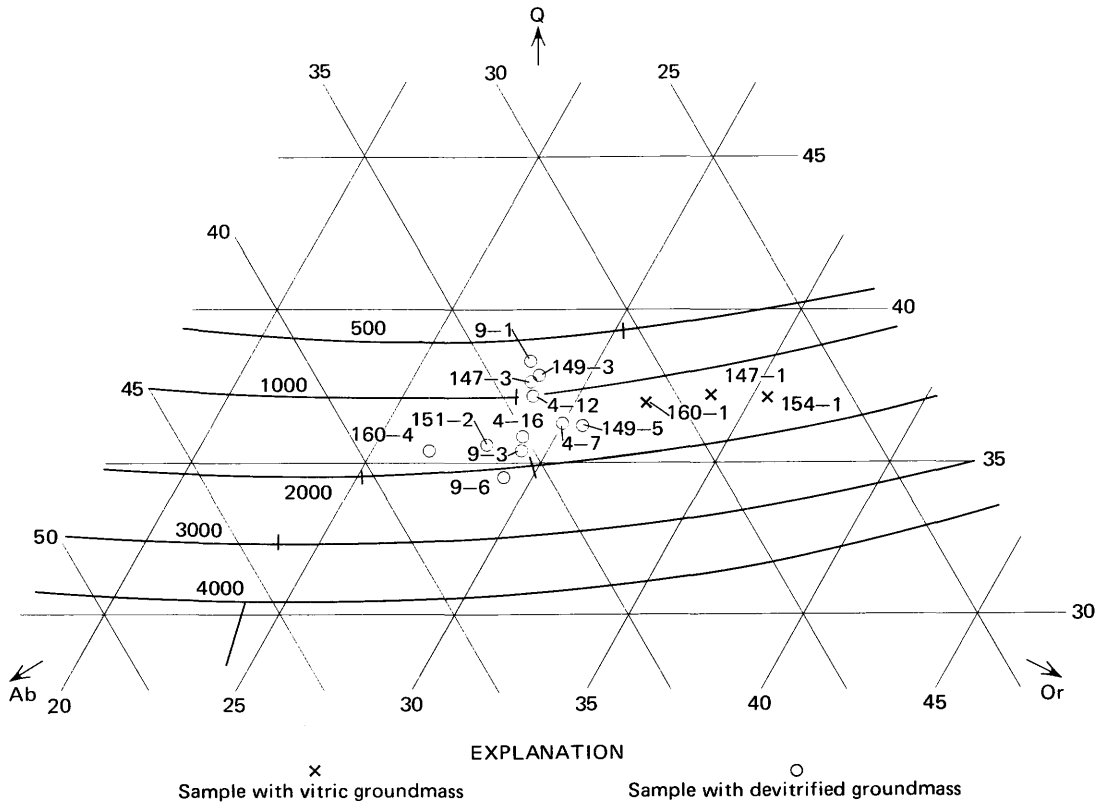

FIGURE 26.—Normative compositions of analyzed samples in the system Q-Or-Ab. Curved lines represent isobaric minima in this system, after Tuttle and Bowen (1958, p. 75), at various water pressures, given in bars. Position of thermal minima indicated by dash or ternary intersection.

cantly from the average. These relationships are illustrated by normative compositions in the system Q-Or-Ab (fig. 27). Phenocryst compositions fall in the bottom part of the diagram and groundmass compositions in the top part. The whole-rock compositions of the samples plot in the center on tielines (not drawn) connecting phenocrysts and groundmass, and cluster closely about the position of the average of the whole-rock samples.

The rocks rich in phenocrysts must be the products of crystallization of the magma now represented by their own groundmasses and could not have formed by crystal settling. If crystal settling had occurred, the whole-rock compositions would vary more. Those rocks that had lost phenocrysts would plot on the opposite side of the average (or "original") composition from the

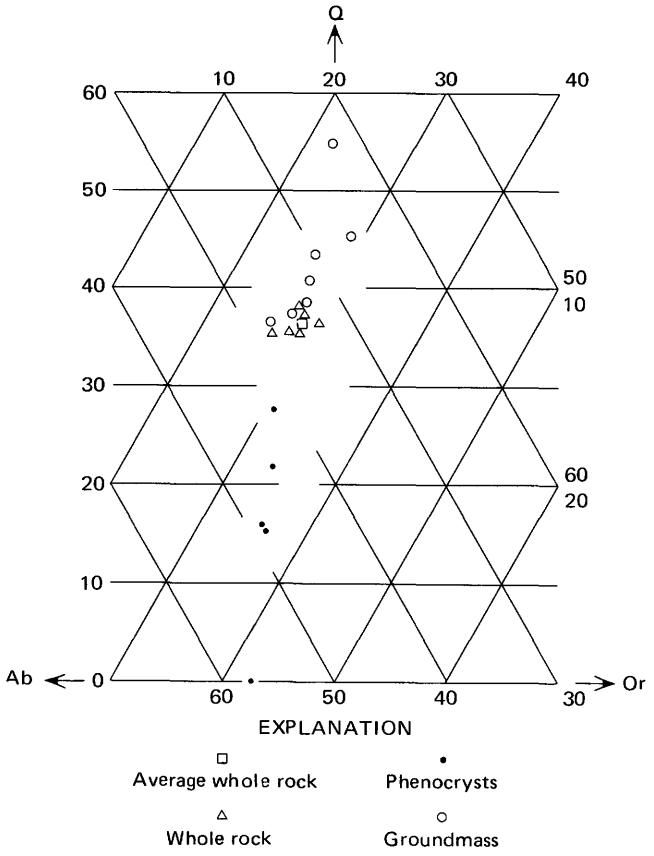

FIGURE 27.—Normative compositions of whole rock, phenocrysts, and groundmass for samples of table 9 in the system Q-Or-Ab.

phenocryst composition, and those that had gained phenocrysts would plot on the side toward the phenocrysts.[2]

INTERPRETATION OF MAGMATIC HISTORY

The welded tuff of Devine Canyon grades upward from a phenocryst-poor base to a phenocryst-rich upper part, but the bulk composition does not vary significantly with the phenocryst content. In this way it differs from the tuffs of southern Nevada (Lipman and others, 1966; Hinrichs and Orkild, 1961; O'Connor, 1963; Noble and others, 1964), most of which grade upward from a crystal-poor rhyolitic base to a crystal-rich quartz latitic cap rock. In the southern Nevada tuffs, the magma chamber was apparently zoned in the reverse sense—rhyolitic at the top, quartz latitic at greater depth.

The Q-Ab-Or diagram for the welded tuff of Devine Canyon (fig. 26) seems at first glance to exhibit a trend in some of the samples, in particular, from samples 9–6 to 9–1. However, although 9–1 is at the base of the Devine Canyon section, it is very rich in phenocrysts and is probably a relatively late eruptive product rather than a sample from the top of magma column (Lipman and others, 1966, p. F42). The others in this "trend" are also in confused order. Most of the variations in the position of points on this diagram are due to variations in content of Al_2O_3 or CaO or in the oxidation state of iron. The method by which norms are calculated causes these factors to affect the Or-Ab ratio and the Q content.

It is apparent from the foregoing that the preeruption magma column was zoned as to phenocryst content but uniform in bulk composition. The lower levels of the column were simply in a more advanced state of crystallization.

Kennedy (1955) points out that water diffuses in a magma chamber so that its chemical potential (for practical purposes, its partial pressure) is uniform throughout. This means that water will be concentrated near the top and edges of the chamber owing to lower temperature, and gradually decrease downward owing to increase in both temperature and confining pressure. It follows that magma will be saturated with water only at the top and edges, and elsewhere will be undersaturated.

Thus, in the Devine Canyon magma, although the increase in temperature with depth would have tended to inhibit crystallization, the accompanying decrease in water content apparently offset this and allowed crystallization to proceed rapidly at depth. Subsequent events leading to eruption followed before enough time had elapsed for significant crystal settling.

The possibility of determining the water pressure obtained just prior to eruption of an ash-flow tuff by use of the experimental data of Tuttle and Bowen (1958) has been considered by Lipman (1966) and Noble (1968). Lipman plots the normative Q-Ab-Or proportions of samples of several compositionally zoned welded tuffs from southern Nevada on the triangular diagram of these components and superposes the isobaric lines and thermal minima of Tuttle and Bowen (1958). The plots (Lipman, 1966, figs. 1–5; Lipman and others, 1966, fig. 26) show a differentiated series following a fractional crystallization path toward a thermal minimum at pressures ranging from 500 to 1,200 bars for several different ash-flow tuffs. He concludes that the positions of the points representing the most silica-rich rocks in these series represent the probable preeruption water pressure.

An important problem, however, is whether or not the ash-flow magmas considered are saturated with

[2]Demonstration of crystallization in place in the magma column has been dependent on the greater feldspar-silica ratio in the phenocrysts than in the groundmass. If the ratio were the same in each, all points on figure 27 would cluster in the center, and whether or not settling had taken place would be indeterminate from considerations in the Q-Or-Ab system.

TABLE 9.—*Average composition of analyzed devitrified tuffs and calculated partial groundmass compositions of selected devitrified tuffs*

Average in percent, 11 devitrified tuffs:

SiO_2	Al_2O_3	Fe_2O_3	FeO	MgO	CaO	Na_2O	K_2O	H_2O^+	H_2O^-	TiO_2	P_2O_5
74.8	11.2	2.5	.57	.26	.44	4.0	4.5	.70	.45	.20	.06

Sample	147–3		151–2		160–4		4–16		149–3		149–5		9–1	
	Groundmass[1]	Difference from whole rock	Groundmass	Difference from whole rock	Groundmass	Difference from whole rock	Groundmass	Difference from whole rock	Groundmass	Difference from whole rock	Groundmass	Difference from whole rock	Groundmass	Difference from whole rock
SiO_2	75.3	+0.1	74.5	+0.3	75.0	−0.3	75.7	+0.6	76.4	+1.0	75.6	+0.3	76.6	+1.4
Al_2O_3	10.6	−.2	10.7	−.3	11.1	−.3	10.4	−1.0	10.0	−1.0	10.7	−1.2	9.0	−2.6
Fe_2O_3[2]	3.4	+.2	3.4	+.2	3.4	+.4	3.5	+.6	3.3	+.6	3.8	+1.3	5.4	+2.0
MgO	.30	+.01	.33	+.02	.20	+.02	.25	+.04	.12	+.02	.16	+.04	.2	+.07
CaO	.26	+.01	.89	+.06	.48	+.05	.5	+.08	.29	+.04	.44	+.13	.35	+.1
Na_2O	4.1	−.1	4.3	0	4.3	0	3.8	−.3	3.7	−.3	3.1	−.6	2.7	−1.0
K_2O	4.3	−.1	4.2	−.1	4.1	−.1	4.3	−.3	4.2	−.3	4.6	−.3	3.4	−1.0
Weight percent alkali feldspar phenocrysts	2.5		6.1		9.3		16.9		16.3		28.3		33.5	
Weight percent quartz phenocrysts	0		1.1		3.6		3.2		3.1		8.0		6.4	

[1]Composition of feldspar from sample WT-6, table 4, utilized in calculation of groundmass compositions.
[2]Total iron expressed as Fe_2O_3.

water. Lipman (1966, p. 824) suggests that Tuttle and Bowen's data (1958) might still be applicable to undersaturated magmas, with the partial pressure of water substituted for total pressure. Water content must then be estimated by other means, and total pressure and depth to the magma chamber can be estimated from a graph such as that which Kennedy (1955, fig. 1) used to show the equilibrium distribution of water in a melt of albite composition.

The near uniformity of composition of the welded tuff of Devine Canyon precludes establishing a differentiation trend by the plotting of points on the Q-Ab-Or diagram (fig. 26, discussion above). However, the cluster of points between about 800 and 1,800 bars suggests crystallization in the magma chamber under a partial water pressure in this range. If the uppermost part of the magma were water saturated, the median value of 1,300 bars would indicate a water content of about 5 percent, a temperature of about 720°C, and a depth to the top of the magma of about 3 miles during crystallization of the phenocrysts. Assuming a uniform partial pressure of water, at greater depths the magma would contain less water, and would be undersaturated (Kennedy, 1955, fig. 1).

The prevalence of resorbed phenocrysts at all levels in the welded tuff of Devine Canyon indicates that the entire magma column was affected by a drop in pressure at some late stage prior to eruption. This pressure drop caused the less dense, liquid, phase to be favored, causing resorption of phenocrysts in a magma undersaturated with water (Noble, 1970a; D. C. Noble, written commun., 1971). Reduction in pressure was probably caused by the ascent of the magma which may have been accompanied by eruption of minor amounts of air-fall tuff. Such tuff is present beneath the ash-flow tuff at the Juntara and Drinkwater Pass sections (154 and 153), and may be covered elsewhere.

When eruption finally occurred, the ash must have flowed onto a very flat plain, judging from the tuff's great areal extent and roughly uniform thickness. Moore's observations (1967) on deposits of the base surge from recent volcanic eruptions show that topography has a strong influence on deposition. The base surge that he observed at Taal Volcano constituted a cold ash flow which must be in many ways analogous to the hotter ash flow or flows which formed the welded tuff of Devine Canyon.

REFERENCES CITED

Baldwin, E. M., 1959, Geology of Oregon: Eugene, Univ. of Oregon, Cooperative Book Store, 136 p.

Berry, L. G., and Thompson, R. M., 1962, X-ray powder data for ore minerals—the Peacock Atlas: Geol. Soc. America Mem. 85, 281 p.

Brown, C. E., and Thayer, T. P., 1966, Geologic map of the Canyon City quadrangle, northeastern Oregon: U.S. Geol. Survey Misc. Geol. Inv. Map I–447, scale 1:250,000.

Brown, G. M., 1960, The effect of ion substitution on the unit cell dimensions of the common clinopyroxenes: Am. Mineralogist, v. 45, nos. 1–2, p. 15–38.

Byers, F. M., Jr. Orkild, P. P., Carr, W. J., and Quinlivan, W. D., 1968, Timber Mountains Tuff, southern Nevada, and its relation to cauldron subsidence: Geol. Soc. America Mem. 110, p. 87–97.

Clark, J. R., Appleman, D. E., and Papike, J. J., 1969, Crystal chemical characterization of clinopyroxenes based on eight new structure refinements, *in* Pyroxenes and amphiboles—Crystal chemistry and phase petrology: Mineralog. Soc. America Spec. Paper 2, p. 31–50.

Deer, W. A., Howie, R. A., and Zussman, J., 1962, Rock-forming minerals, v. 2, Chain silicates: London, Longmans, Green and Co., 379 p.

Evernden, J. F., Savage, D. E., Curtis, G. H., and James, G. T., 1964, Potassium-argon dates and the Cenozoic mammalian chronology of North America: Am. Jour. Sci., v. 262, p. 145–198.

Fisher, R. V., 1966, Mechanism of deposition from pyroclastic flows: Am. Jour. Sci., v. 264, no. 5, p. 350–363.

Greene, R. C., 1972, Generalized geologic map of the Burns and West Myrtle Butte 15-minute quadrangles, Oregon: U.S. Geol. Survey Misc. Geol. Inv. Map I–680.

Greene, R. C., Walker, G. W., and Corcoran, R. E., 1972, Geologic map of the Burns (AMS) quadrangle, Oregon: U.S. Geol. Survey Misc. Geol. Inv. Map I–680.

Haddock, G. H., 1967, The Dinner Creek welded ash-flow tuff of the Malheur Gorge area, Malheur County, Oregon: Eugene, Univ. of Oregon, Ph. D. thesis, 111 p.

Hess, H. H., 1949, Chemical composition and optical properties of common clinopyroxenes, pt. I: Am. Mineralogist, v. 34, nos. 9–10, p. 621–666.

Hinrichs, E. N., and Orkild, P. P., 1961, Eight members of the Oak Spring formation, Nevada Test Site and vicinity, Nye and Lincoln Counties, Nevada, *in* Geological Survey research, 1961: U.S. Geol. Survey Prof. Paper 424–D, p. D96–D103.

Kennedy, G. C., 1955, Some aspects of the role of water in rock melts, *in* Poldervaart, Arie, ed., Crust of the earth—a symposium: Geol. Soc. America Spec. Paper 62, p. 489–503.

Kittleman, L. R., Green, A. R., Haddock, G. H., Hagood, A. R., Johnson, A. M., McMurray, J. M. Russell, R. G., and Weeden, D. A., 1967, Geologic map of the Owyhee region, Malheur County, Oregon: Oregon Univ. Mus. Nat. History Bull. 8, scale 1:125,000.

Kittleman, L. R., Green, A. R., Hagood, A. R., Johnson, A. M., McMurray, J. M., Russell, R. G., and Weeden, D. A., 1965, Cenozoic stratigraphy of the Owyhee region, southeastern Oregon: Oregon Univ. Mus. Nat. History Bull. 1, 45 p.

Lipman, P. W., 1965, Chemical comparison of glassy and crystalline volcanic rocks: U.S. Geol. Survey Bull. 1201–D, p. D1–D23.

———1966, Water pressures during differentiation and crystallization of some ash-flow magmas from southern Nevada: Am. Jour. Sci., v. 264, no. 10, p. 810–826.

Lipman, P. W., and Christiansen, R. L., 1964, Zonal features of an ash-flow sheet in the Piapi Canyon Formation, southern Nevada *in* Geological Survey research, 1964: U.S. Geol. Survey Prof. Paper 501–B, p. B74–B78.

Lipman, P. W., Christiansen, R. L., and O'Connor, J. T., 1966, A compositionally zoned ash-flow sheet in southern Nevada: U.S. Geol. Survey Prof. Paper 524–F, p. F1–F47.

Lipman, P. W., Christiansen, R. L., and Van Alstine, R. E., 1969, Retention of alkalis by calc-alkalic rhyolites during crystallization and hydration: Am. Mineralogist, v. 54, p. 286–291.

Moore, J. G., 1967, Base surge in recent volcanic eruptions: Bull. Volcanol., v. 30, p. 337–363.

Noble, D. C., 1968, Calcium contents, Na_2O:K_2O ratios, and water contents of the Paintbrush and Timber Mountain magmas: Am. Jour. Sci., v. 266, p. 860–864.

———1970a, Significance of phenocryst resorption for the intratelluric crystallization and eruptive history of silicic pyroclastic rocks [abs.]: Geol. Soc. America, Abs. with Programs, v. 2, no. 2, p. 125.

———1970b, Loss of sodium from crystallized comendite welded tuffs of the Miocene Grouse Canyon Member of the Belted Range Tuff, Nevada: Geol. Soc. America Bull., v. 81, p. 2677–2688.

Noble, D. C., Anderson, R. E., Ekren, E. B., O'Connor, J. T., 1964, Thirsty Canyon Tuff of Nye and Esmeralda Counties, Nevada, *in* Geological Survey research, 1964: U.S. Geol. Survey Prof. Paper 475–D, p. D24–D27.

O'Connor, J. T., 1963, Petrographic characteristics of some welded tuffs of the Piapi Canyon Formation, Nevada Test Site, Nevada, *in* Geological Survey research, 1963: U.S. Geol. Survey Prof. Paper 475–B, p. B52–B55.

Piper, A. M., Robinson, T. W., and Park, C. F., 1939, Geology and ground-water resources of the Harney Basin, Oregon: U.S. Geol. Survey Water-Supply Paper 841, 189 p.

Poldervaart, Arie, and Hess, H. H., 1951, Pyroxenes in the crystallization of basaltic magma: Jour. Geology, v. 59, no. 5, p. 472–489.

Rittmann, A., 1952, Nomenclature of volcanic rocks: Bull. Volcanol., ser. 2, v. 12, p. 75–102.

Ross, C. S., and Smith, R. L., 1961, Ash-flow tuffs—Their origin, geologic relations and identification: U.S. Geol. Survey Prof. Paper 366, 81 p.

Shapiro, Leonard, 1967, Rapid analysis of rocks and minerals by a single-solution method, *in* Geological Survey research, 1967: U.S. Geol. Survey Prof. Paper 575–B, p. B187–B191.

Shapiro, Leonard, and Brannock, W. W., 1962, Rapid analysis of silicate, carbonate, and phosphate rocks: U.S. Geol. Survey Bull. 1144–A, 56 p.

Smith, J. V., and MacKenzie, W. S., 1958, The cooling history of high-temperature sodium-rich feldspars, pt. 4 *of* The alkali feldspars: Am. Mineralogist, v. 43, nos. 9–10, p. 872–889.

Smith, R. L., 1960a, Ash flows: Geol. Soc. America Bull., v. 71, no. 6, p. 795–841.

———1960b, Zones and zonal variations in welded ash flows: U.S. Geol. Survey Prof. Paper 354–F, p. 149–159.

Swanson, D. A., 1969, Reconnaissance geologic map of the east half of the Bend quadrangle, Crook, Wheeler, Jefferson, Wasco, and Deschutes Counties, Oregon: U.S. Geol. Survey Misc. Geol. Inv. Map I–568, scale 1:250,000.

Tuttle, O. F., and Bowen, N. L., 1958, Origin of granite in the light of experimental studies in the system $NaAlSi_3O_8$–$KAlSi_3O_8$–SiO_2–H_2O: Geol. Soc. America Mem. 74, 153 p.

Walker, G. W., 1963, Reconnaissance geologic map of the eastern half of the Klamath Falls (AMS) quadrangle, Lake and Klamath Counties, Oregon: U.S. Geol. Survey Mineral Inv. Field Studies Map MF–260, scale 1:250,000.

———1969, Geology of the High Lava Plains province, *in* Mineral and water resources of Oregon: Oregon Dept. Geology and Mineral Industries Bull. 64, p. 77–79.

———1970, Cenozoic ash-flow tuffs of Oregon: The Ore Bin, v. 32, no. 6, p. 97–115.

Walker, G. W., Peterson, N. V., and Greene, R. C., 1967 Reconnaissance geologic map of the east half of the Crescent quadrangle, Lake, Deschutes, and Crook Counties, Oregon: U.S. Geol. Survey Misc. Geol. Inv. Map I–493, scale 1:250,000.

Walker, G. W., and Repenning, C. A., 1965, Reconnaissance geologic map of the Adel quadrangle, Lake, Harney, and Malheur Counties, Oregon: U.S. Geol. Survey Misc. Geol. Inv. Map I–446, scale 1:250,000.

☆ U.S. GOVERNMENT PRINTING OFFICE: 1973—515–657/44